SAND2018-10040C

DNS of Turbulent Combustion in Complex Flows

UK Consortium on Turbulent Reacting Flows Annual Meeting

Office of Science
U.S. Department of Energy

Selwyn College
Cambridge University
September 12-13, 2018

GAS PHASE CHEMICAL PHYSICS

Motivation

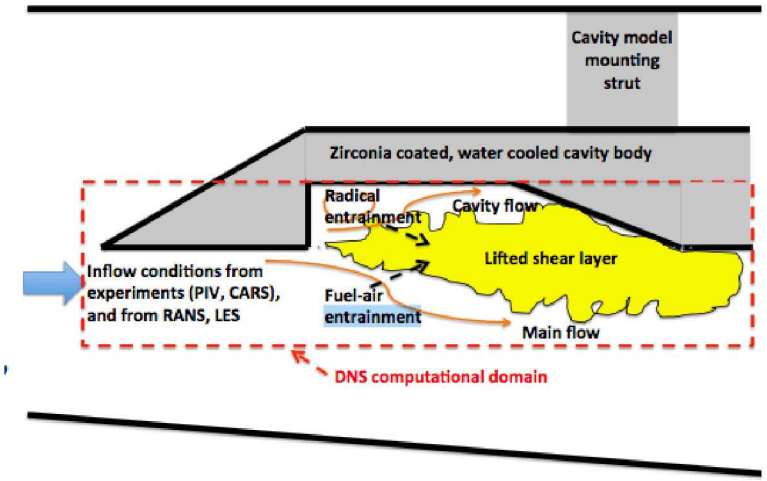

Experiments
PIV, PLIF
(UVa, GWU, NASA)

Early injection PCCI

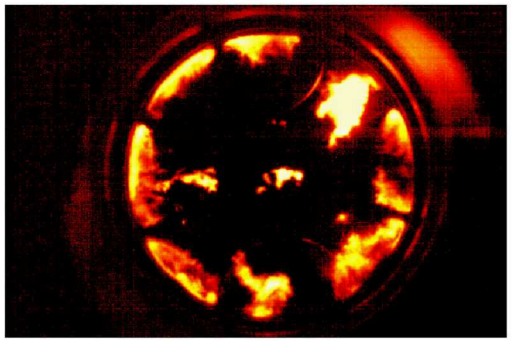

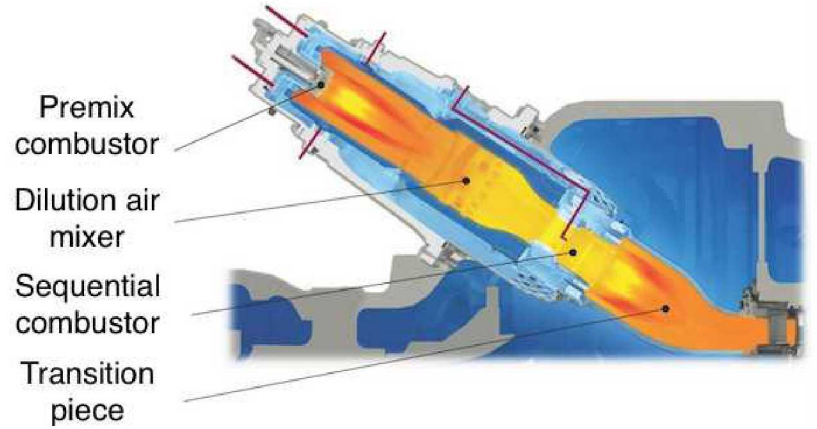

Gain insights into:

- Flame stabilization mechanism
- Effect of heat release
- Turbulence-chemistry interactions

DNS of Flame Propagation and Structure Behind a Backwards Facing Step

A. Konduri, H. Kolla, and J. H. Chen

Sandia National Laboratories

Office of Science
U.S. Department of Energy

GAS PHASE CHEMICAL PHYSICS

S3D - multiblock

Multiblock construction

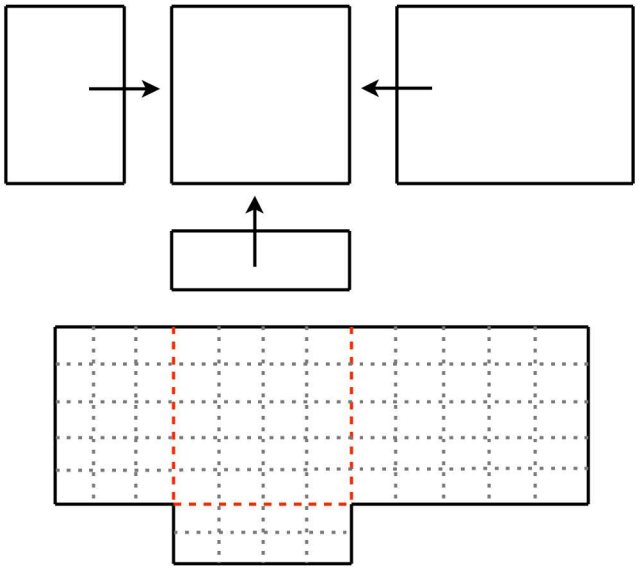

Weak scaling on Titan

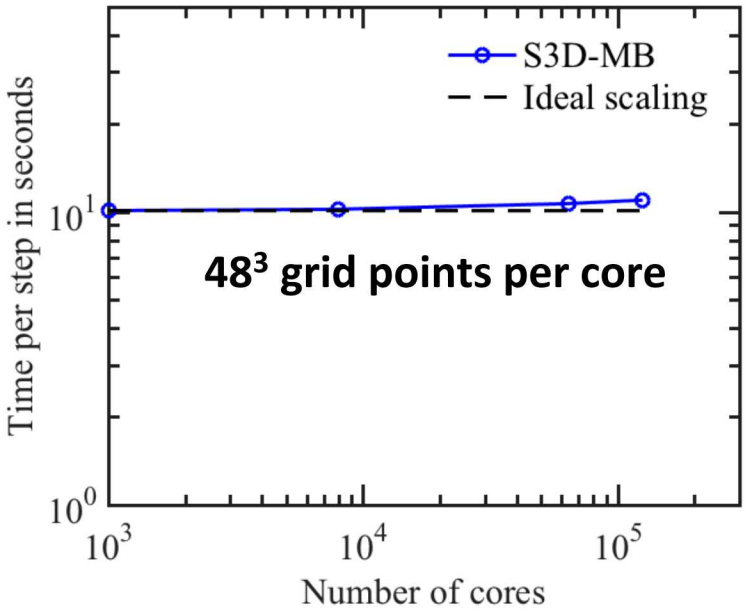

Sample from 2D simulation

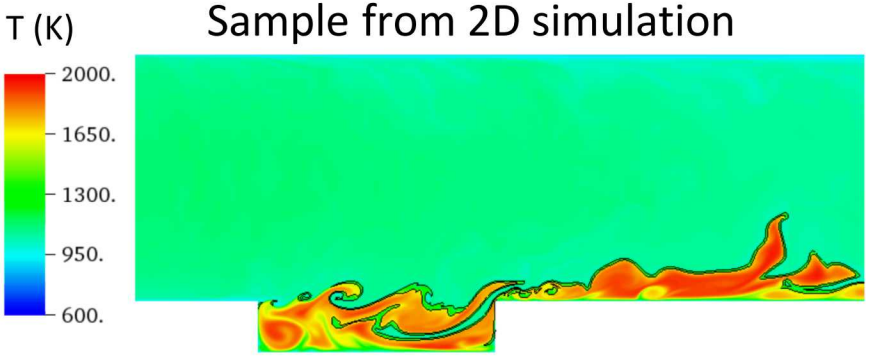

With IBM

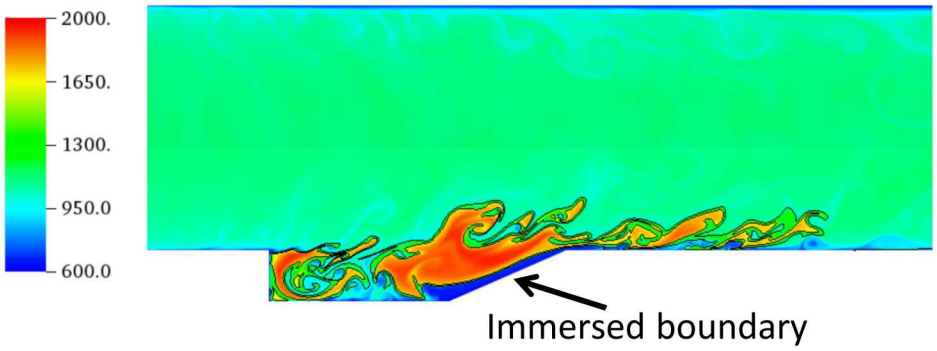

Backward-facing step

Ethylene-air
Φ = 0.42
U = 200 m/s
u’ = 10%
T = 1125 K

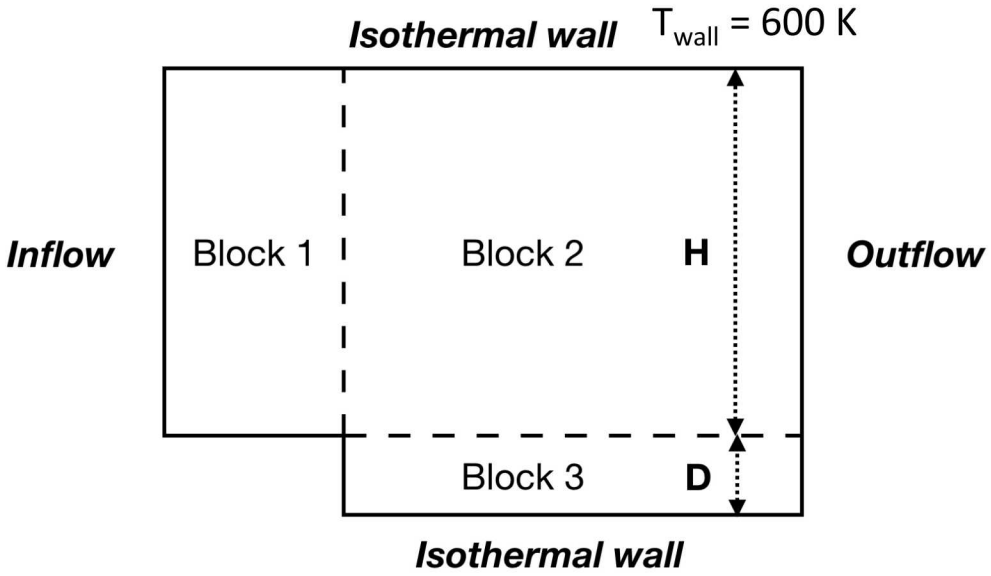

H	1.47 cm
D	0.3048 cm
Re_H	35000
Re_T	788
Grid count	2.6 billion
CPU hrs	25 million

- **Mechanism:** 22 species non-stiff reduced ethylene-air (Lu et al. 2012)
- **Transport model:** mixture averaged
- **Turbulent inflow profile:** feed data generated from a separate 3D DNS of channel

Results

Vorticity magnitude

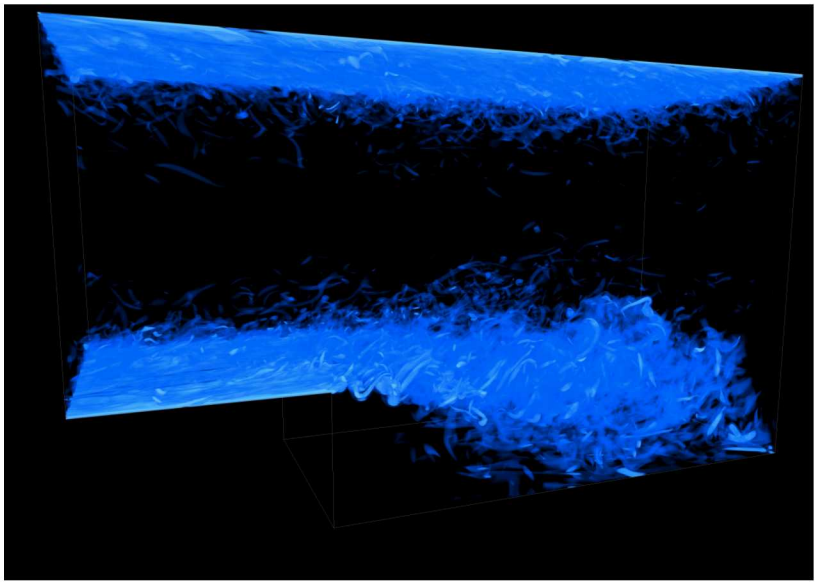

Heat release rate

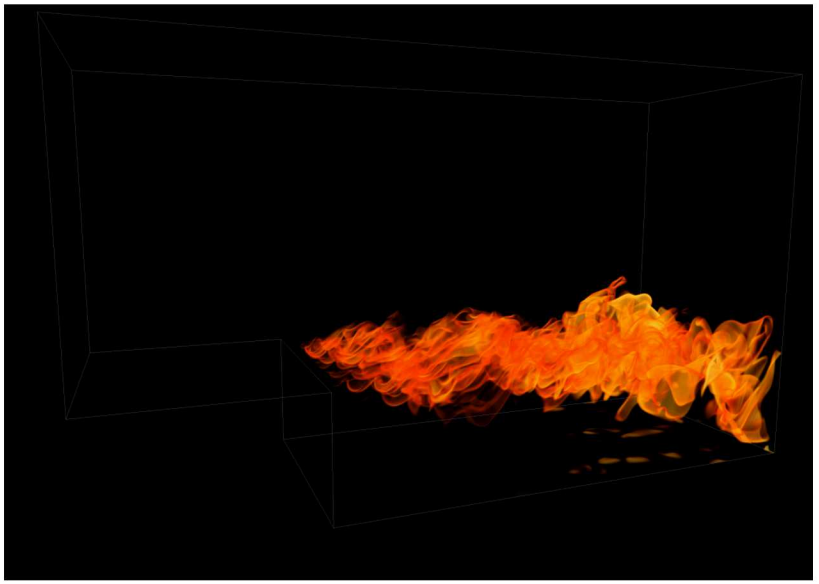

Vorticity dynamics

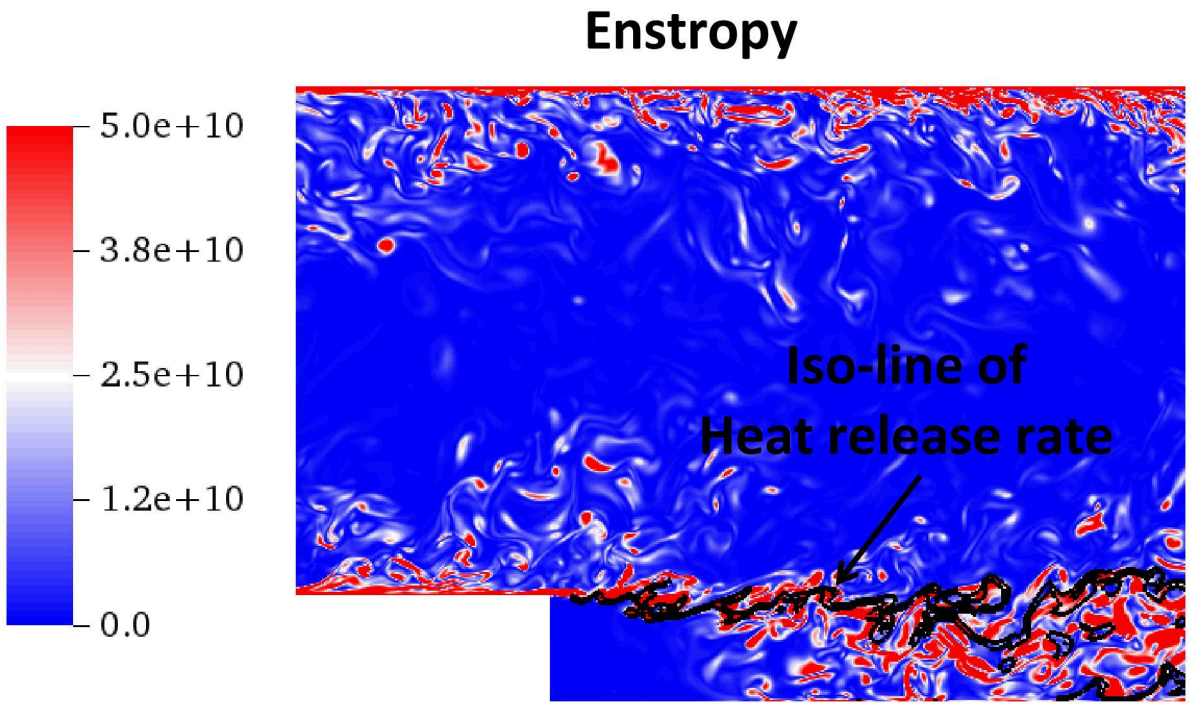

- Enstrophy present dominantly on product side

Vorticity dynamics

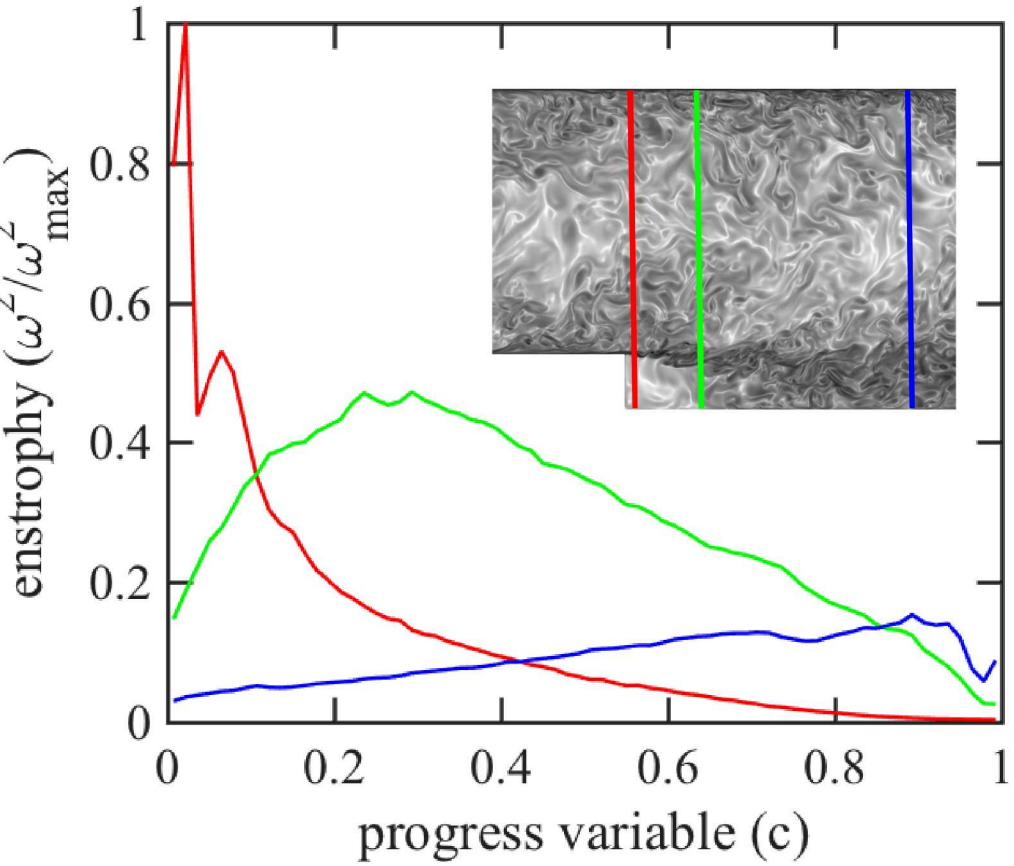

Flame stabilization

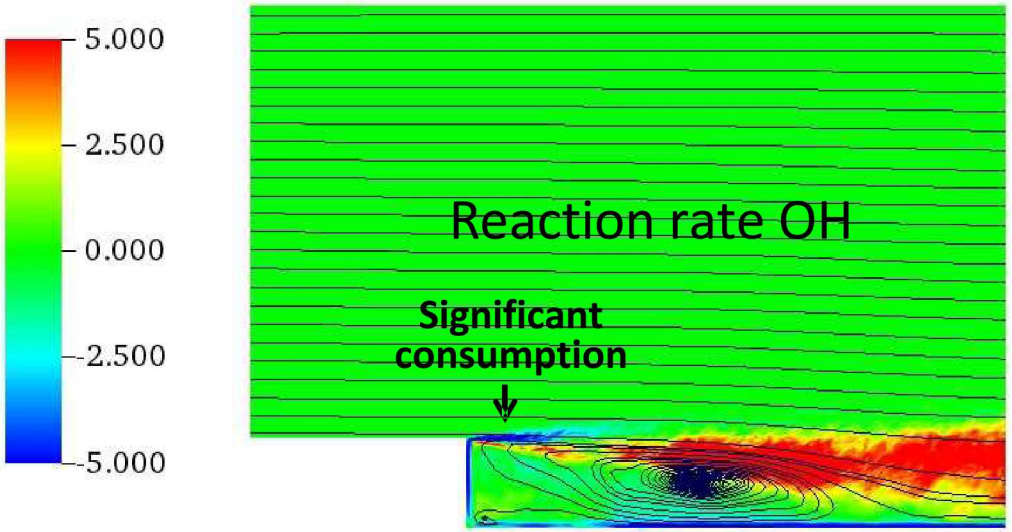

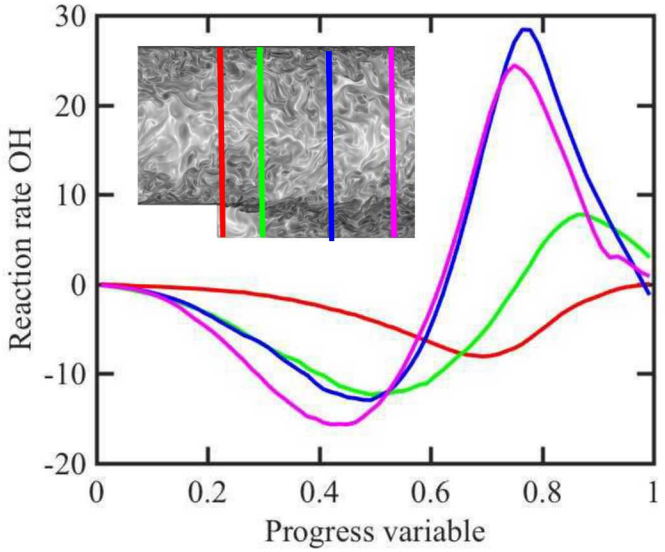

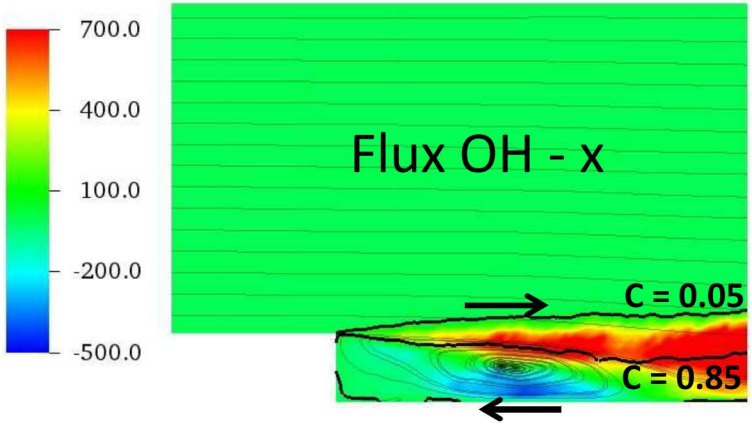

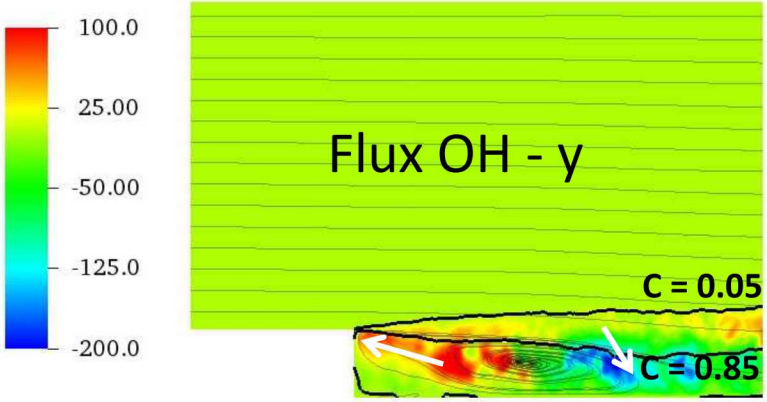

Flame structure

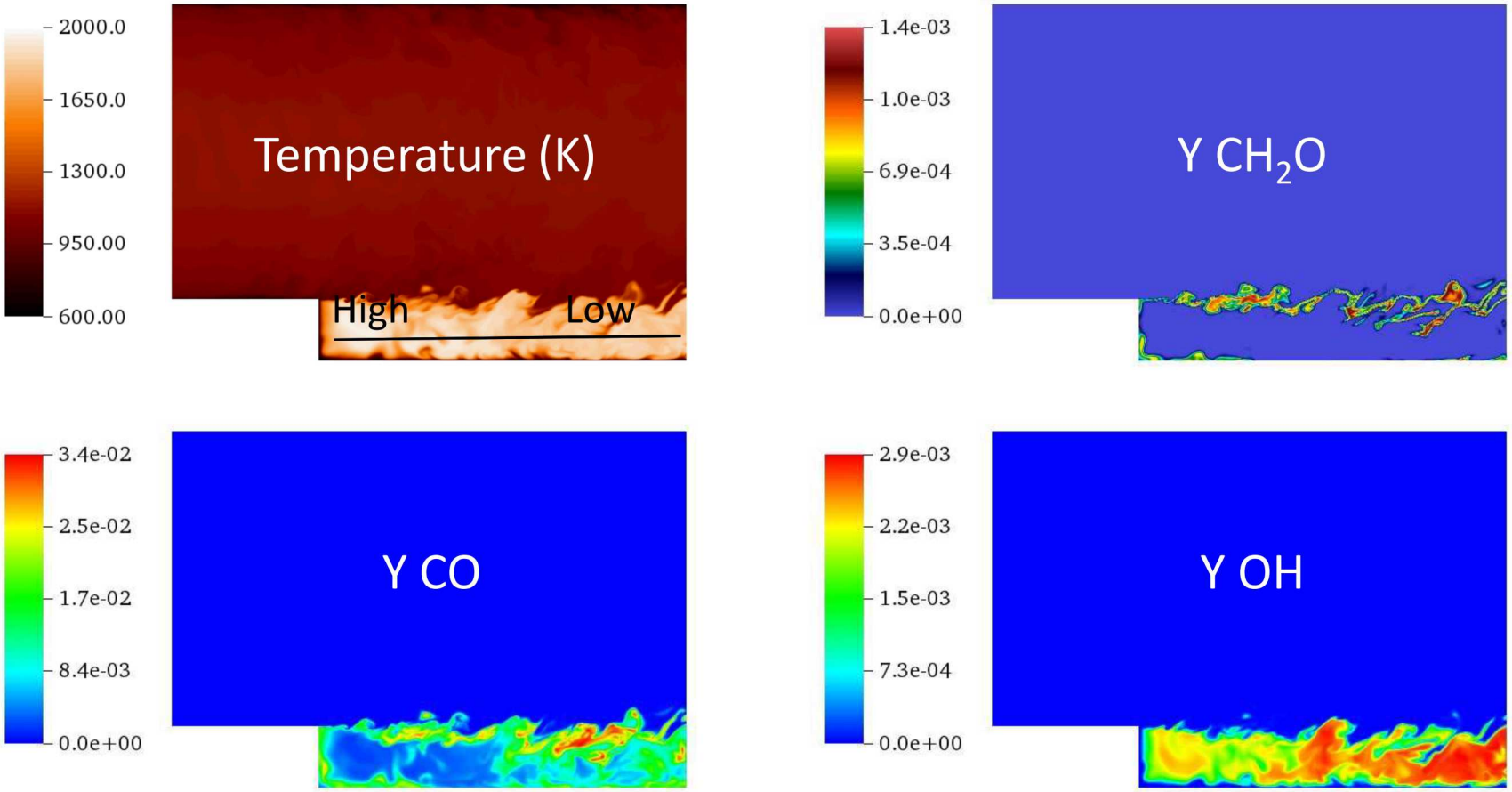

- Flame structure varies with distance from the step
- Flame-flame interaction present due to the shear
- Incomplete oxidation

Flame structure

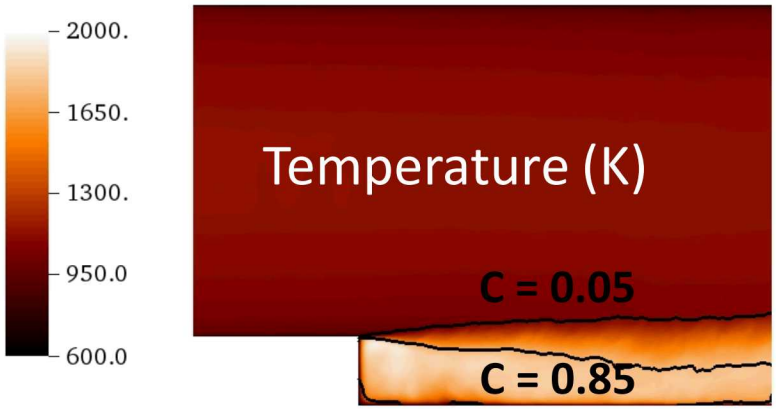

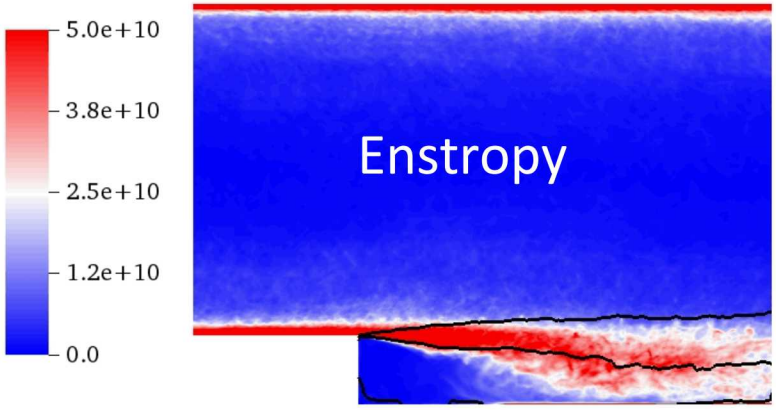

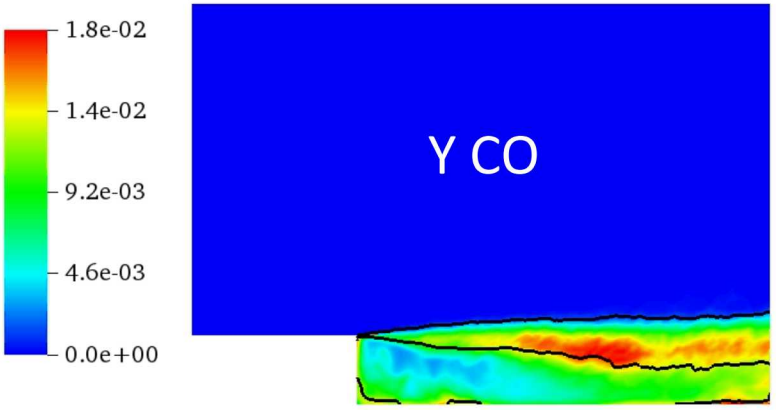

Flame structure

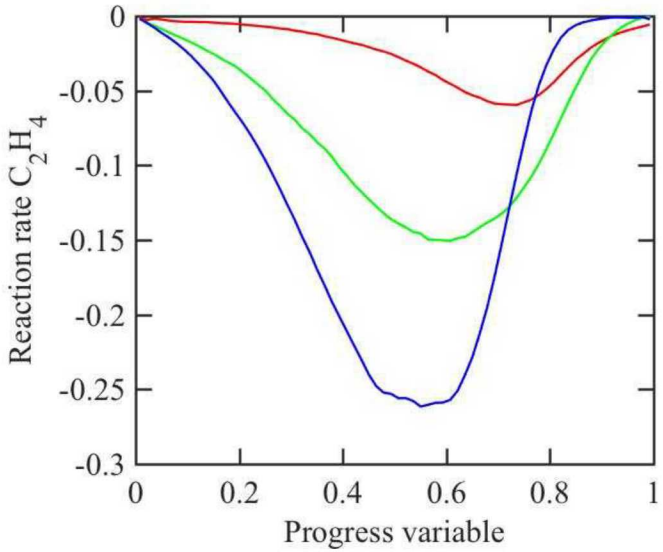

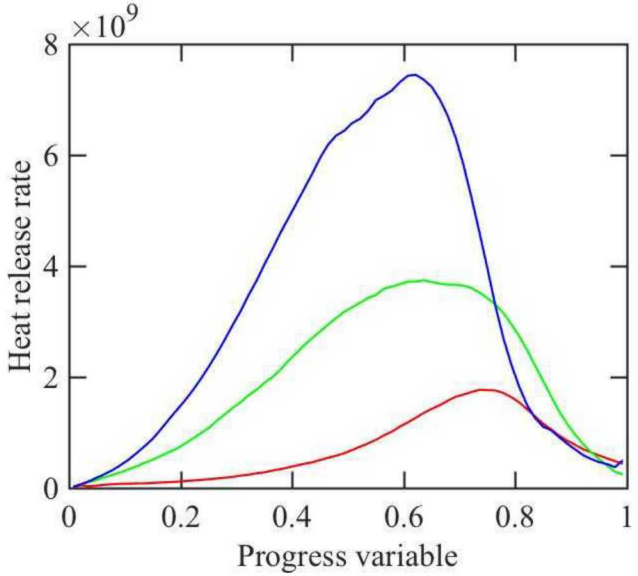

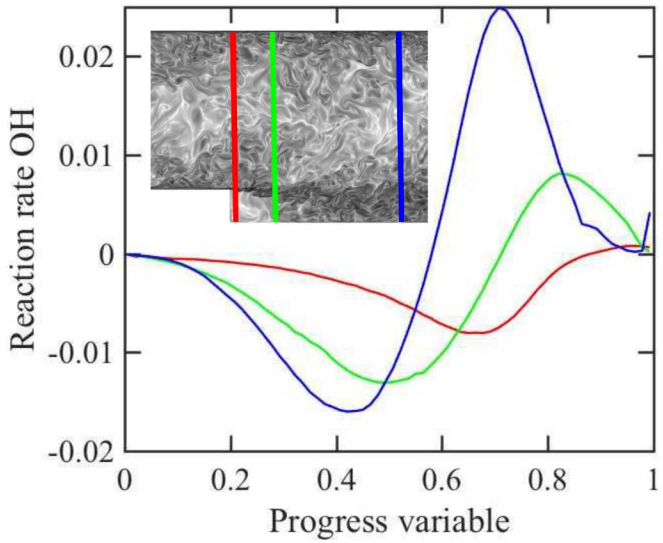

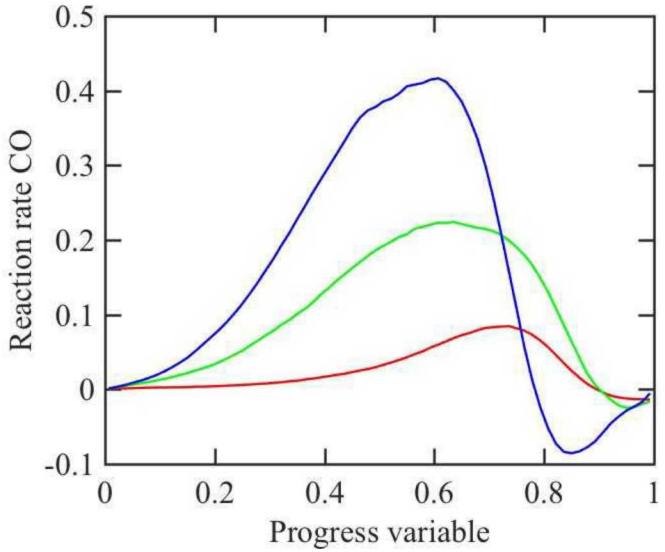

Summary

- DNS of C2H4/air flame stabilization behind a backwards facing step
- Strong interaction between recirculation zone, shear layer, and flame brush
- Radicals from the recirculation zone assist in anchoring the flame
- Turbulence generation migrates towards products downstream of the stabilization point
- Implications for modifications to flame structure and heat losses to the wall

Direct Numerical Simulation of flame stabilization assisted by auto-ignition at *reheat* conditions

Konduri Aditya[a], Andrea Gruber[b] and Jacqueline H. Chen[a]

[a]Combustion Research Facility, Sandia National Laboratories, Livermore, CA, USA
[b]SINTEF Energy Research, Trondheim, Norway

Acknowledgements:
Basic Energy Sciences, Office of Science, DOE
OLCF, NERSC, Norwegian CCS Research Centre (NCCS)

Staged gas turbine combustion

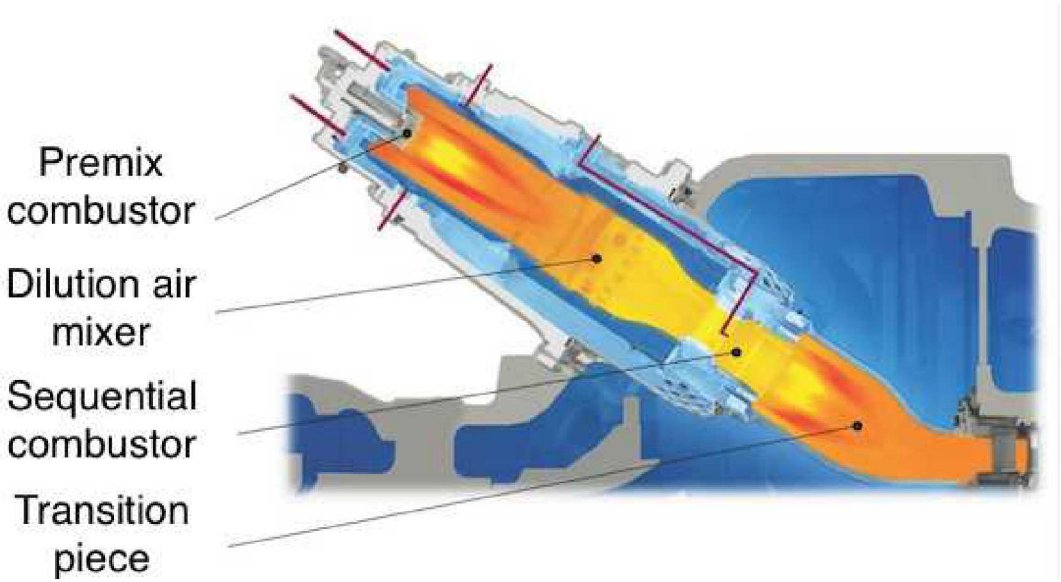

- Originally developed by ABB for high efficiency, load flexibility and low emissions
- Recently improved and simplified (reduced cost) for the H-class GT36
- First (premix) combustion stage based on flame propagation
- Second (sequential) combustion stage based on auto-ignition

Staged gas turbine combustion

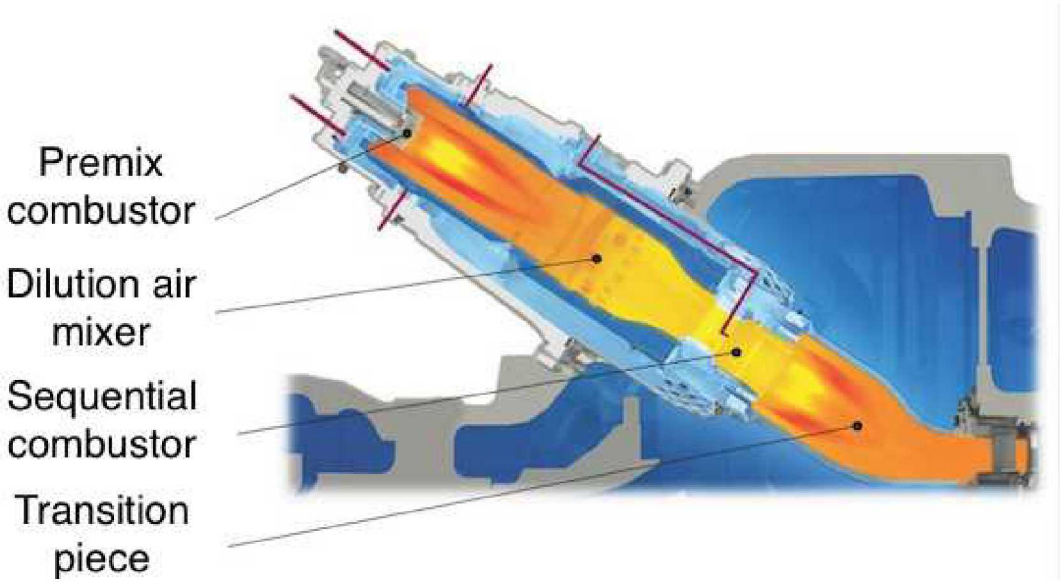

- Originally developed by ABB for high efficiency, load flexibility and low emissions
- Recently improved and simplified (reduced cost) for the H-class GT36
- First (premix) combustion stage based on flame propagation
- Second (sequential) combustion stage based on auto-ignition

Staged gas turbine combustion

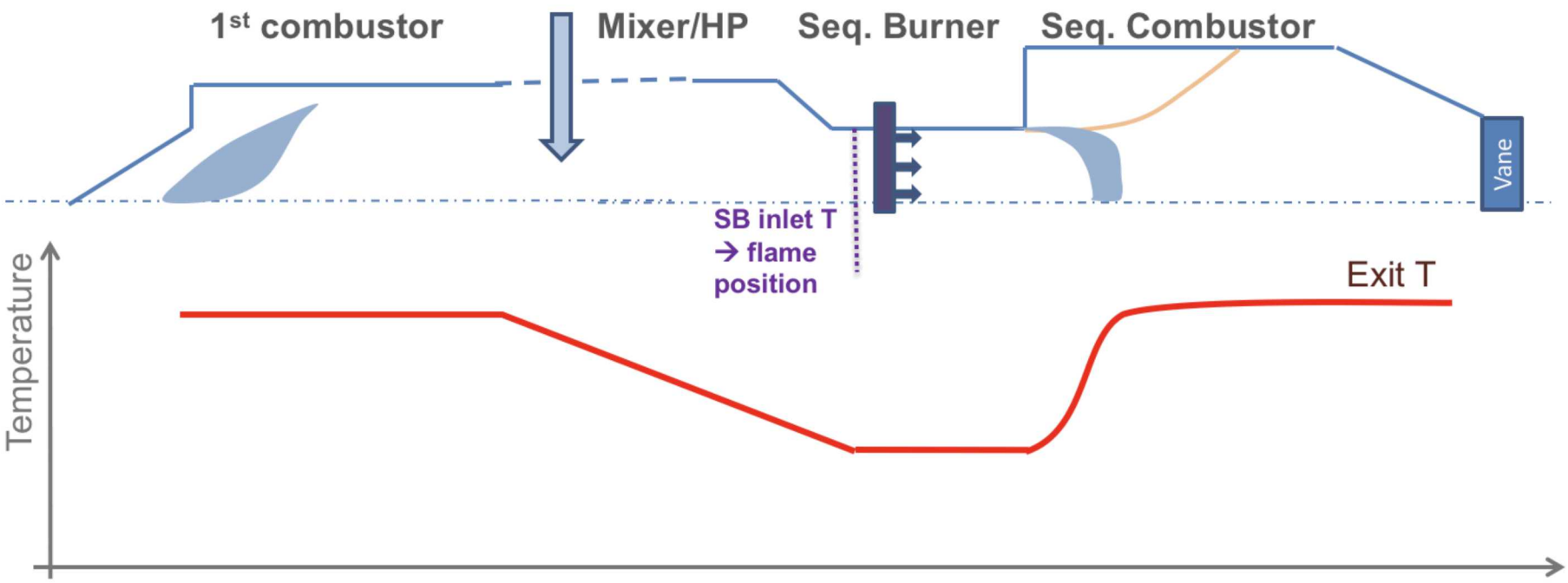

- Adjusting firing temperature of 1st stage allows control of t_{ign} in 2nd stage

Staged gas turbine combustion

Hydrogen fuel

- Flashback in 1st stage
- Early auto-ignition in 2nd stage

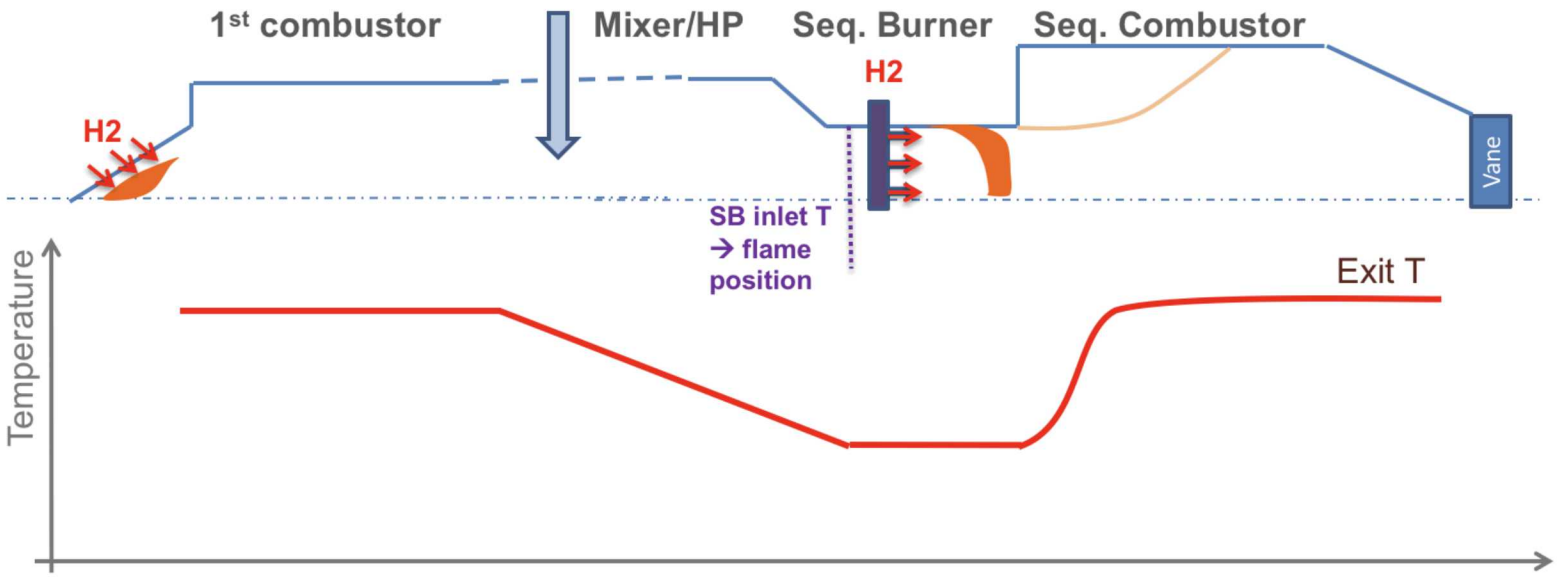

- 2nd stage is mainly auto-ignition stabilized
- 2nd stage inlet temperature needs to be decreased and not 2nd stage flame temperature

Staged gas turbine combustion

Hydrogen fuel

- Flashback in 1st stage
- Early auto-ignition in 2nd stage

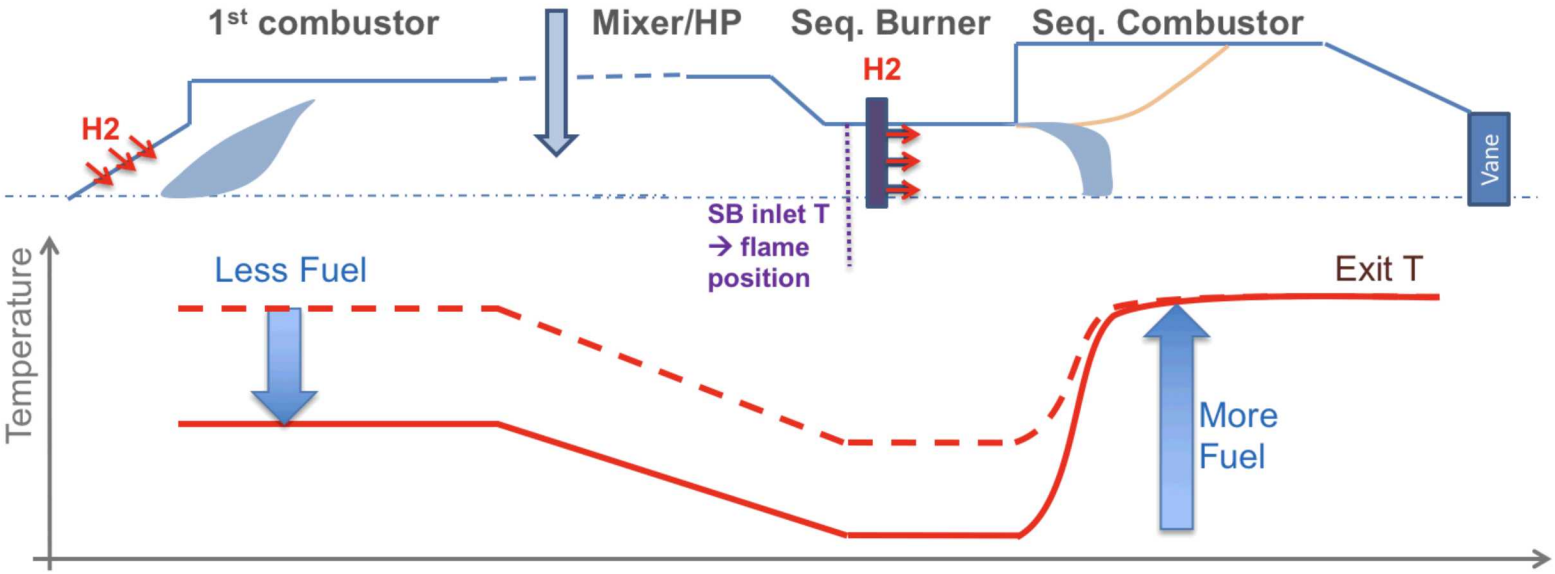

- 2nd stage is mainly auto-ignition stabilized
- 2nd stage inlet temperature needs to be decreased and not 2nd stage flame temperature
- 1st stage de-rating is compensated by shifting fuel to 2nd stage

Reheat burner

DNS of idealized reheat burner configuration from Ansaldo Energia

Operating conditions:

- Inlet temperature: ~ 1100 K
- Pressure: ~ 20 atm

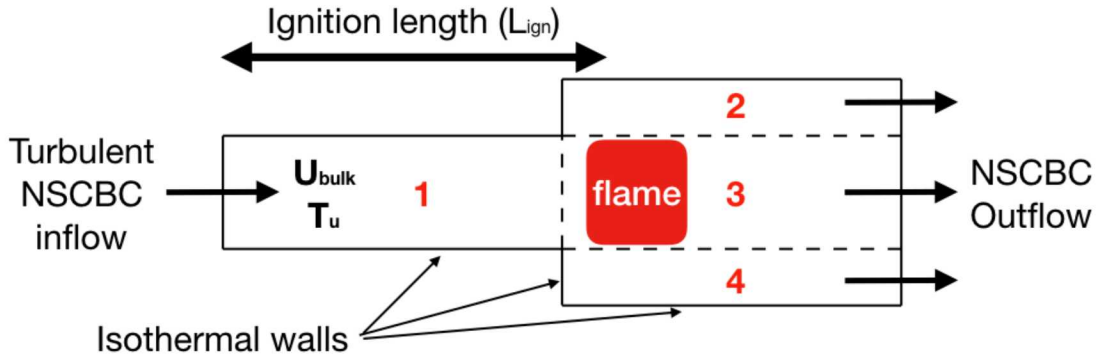

Scaled conditions:

- Mean inlet temperature:
- Pressure: 1 atm
- Fuel: hydrogen

Objective:

- Understand the flame stabilization
- Identify the modes of combustion
- Quantify the role of auto ignition

S3D - Multiblock

- Mildly complex geometry enabled by multi-block DNS capability
- Construct geometries by assembling several cuboidal blocks (like Lego)
- Compressible formulation (J. H. Chen et al., CSD 2009)
- Spatial derivatives: 8th order CD schemes & 10th order filter
- Time integration: 4th order Runge-Kutta
- Mixture averaged transport model

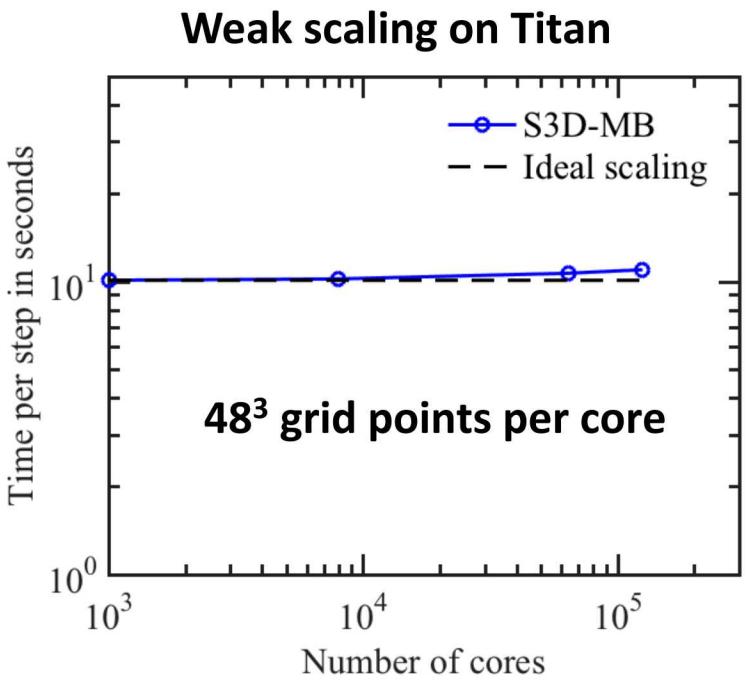

Code scales well on hundreds of thousands of processors

Simulation details

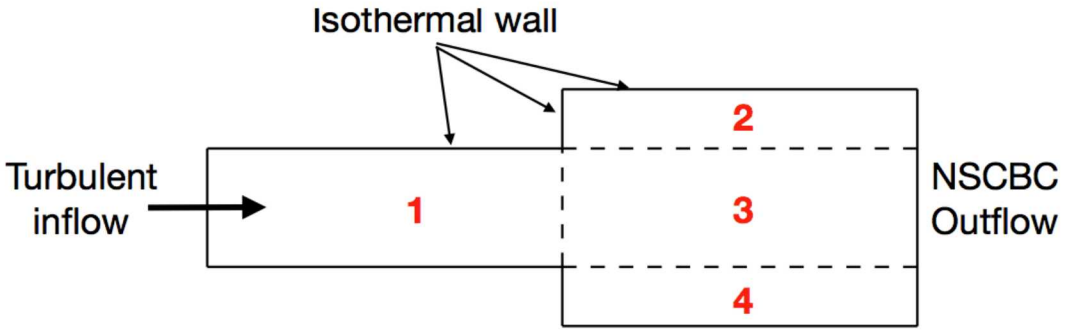

1.25 billion grid points
20 million CPU hours
$Re_b = 13000$

- **Chemical mechanism:** 9 species hydrogen-air (Li et al., 2004)
- **Inflow composition:** premixed H2 + O2 + N2 + H2O (ϕ = 0.35)
- Ubulk = 200m/s, u' = 20m/s, T_{inlet} = 1100K, T_{wall} = 750K
- **Inflow profile:** feed from DNS of a fully developed channel flow

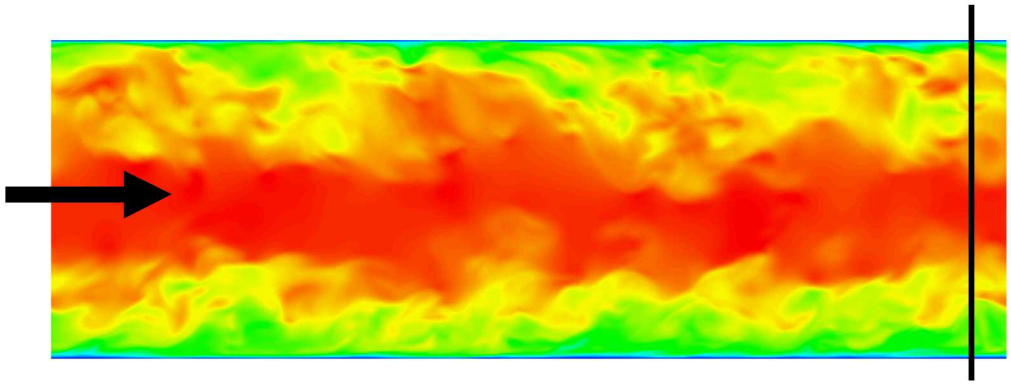

Iso-surfaces of vorticity magnitude colored by temperature

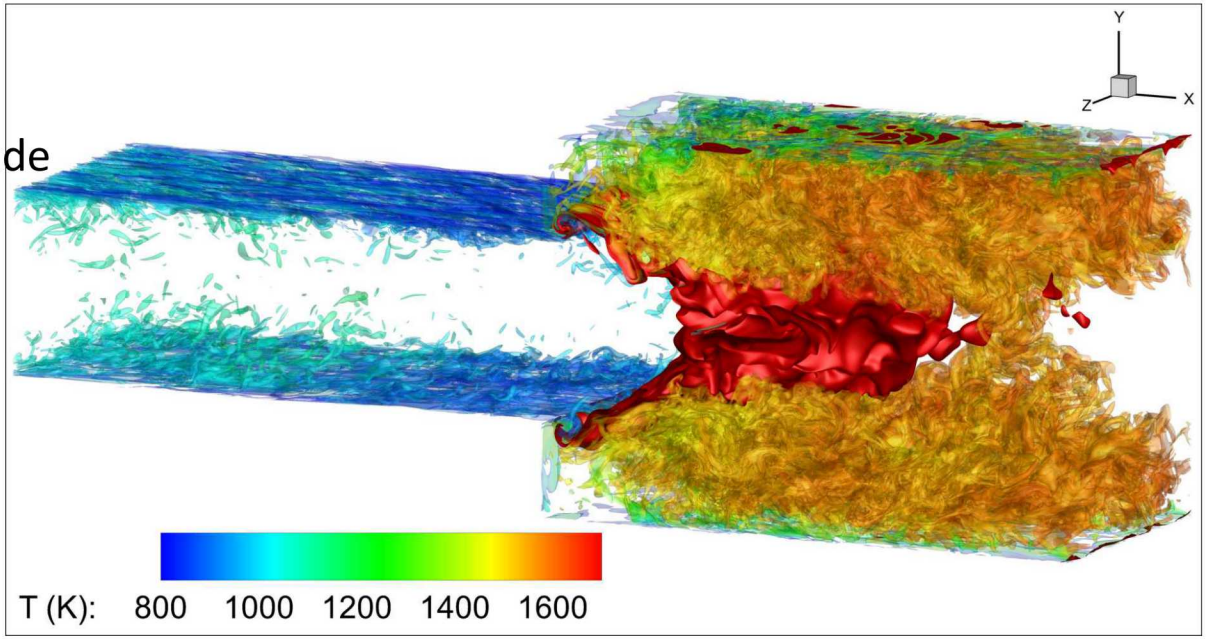

Two combustion configurations are observed:

- Design state: mainly auto-ignition in the combustion chamber
- Intermittent auto-ignition state: ignition in mixing section

Design combustion state

Heat release rate

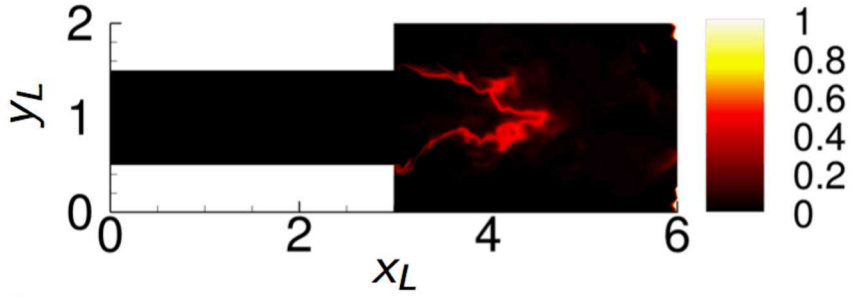

Temperature

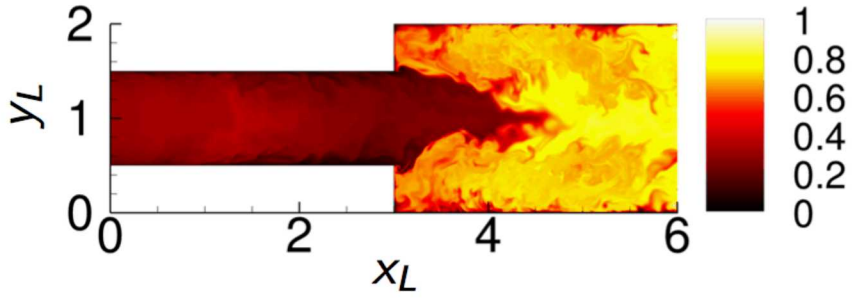

Mass fraction of HO_2

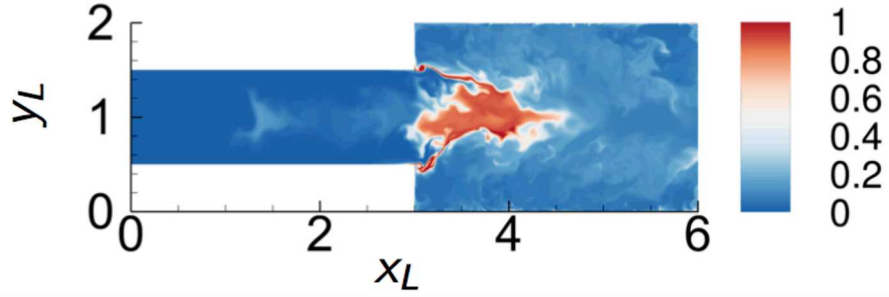

Combustion modes:

- Autoignition along center-line
- Flame propagation near corners
- HO2: indicative of chain branching

Transport budget analysis

$$\frac{\partial(\rho Y_{OH})}{\partial t} = -\nabla_\beta \cdot (\rho Y_{OH}\mathbf{u}_\beta) - \nabla_\beta \cdot (\rho Y_{OH}\mathbf{V}_{\beta,OH}) + W_{OH}\dot{\omega}_{OH}$$

Advection Diffusion Reaction

- Auto-ignition: balance between advection and reaction
- Flame propagation: balance between diffusion and reaction

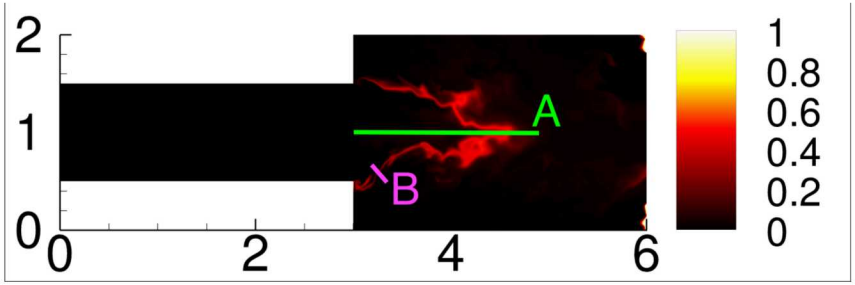

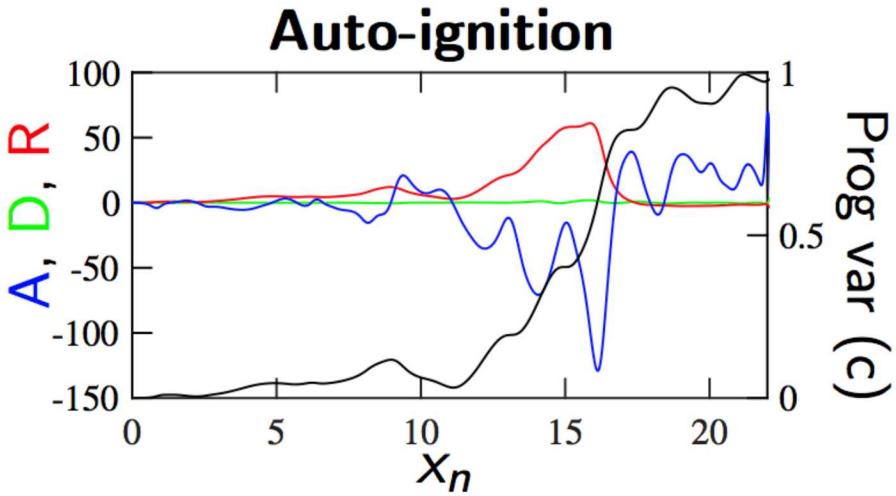

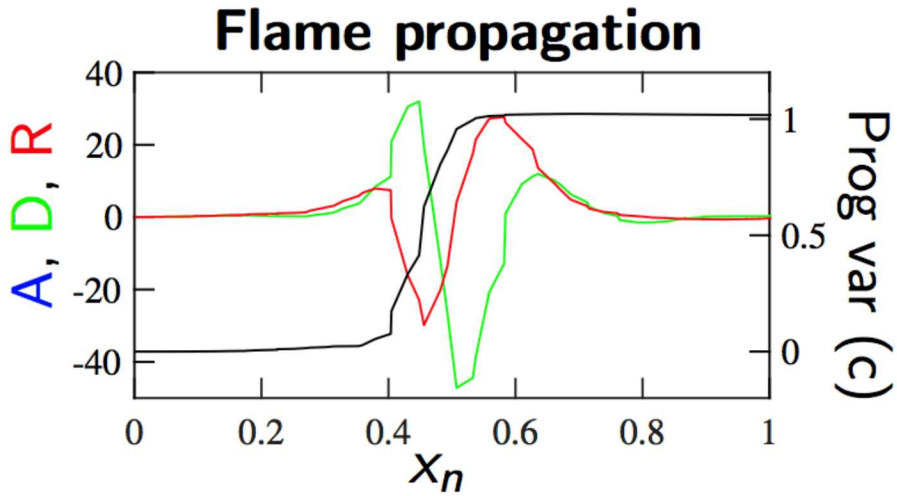

Chemical Explosive Mode Analysis

- $\alpha = \phi s / \phi \omega$: ratio of the projected non-chemical source term and the projected chemical source term (C. Xu et al., PROCI 2018)

Three mode are identified:

- Assisted-ignition ($\alpha > 1$): diffusion significantly promotes reaction
- Auto-ignition ($-1 < \alpha < 1$): chemistry plays a dominant role
- Extinction zone ($\alpha < -1$): diffusion dominates chemistry and suppresses ignition

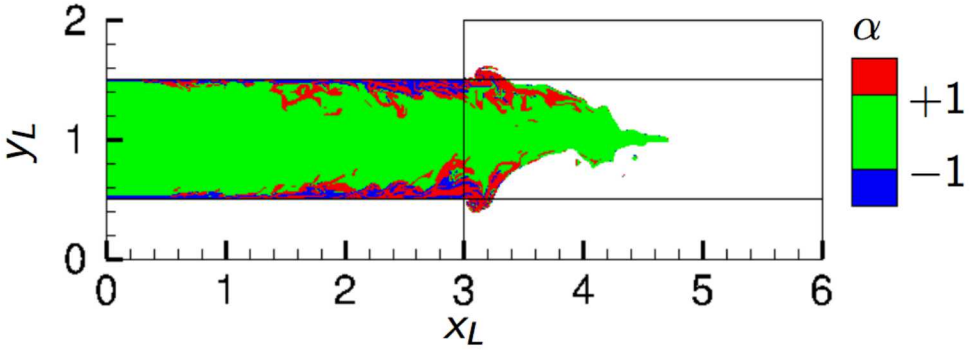

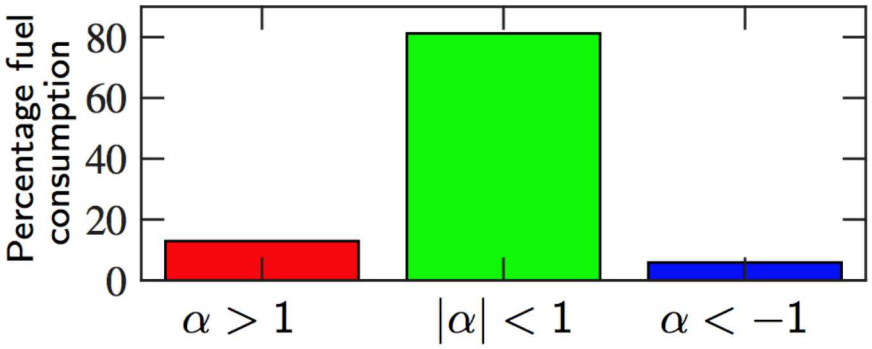

Intermittent auto-ignition state

Heat release rate

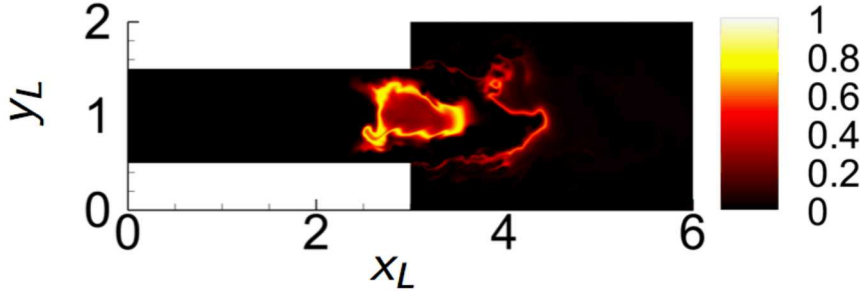

Temperature

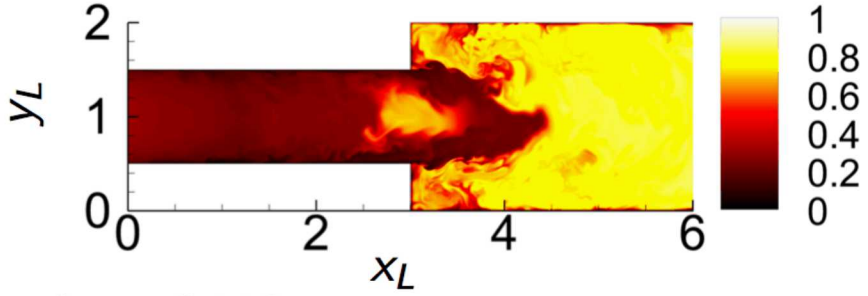

Mass fraction of HO_2

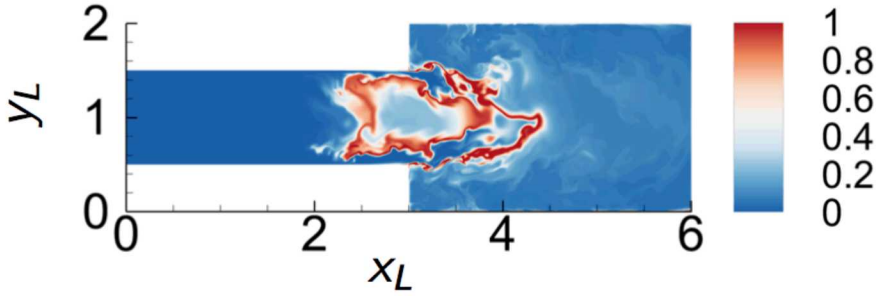

- Early auto-ignition in the mixing section
- Ignition kernel advects downstream
- Occurs intermittently

Intermittent auto-ignition state

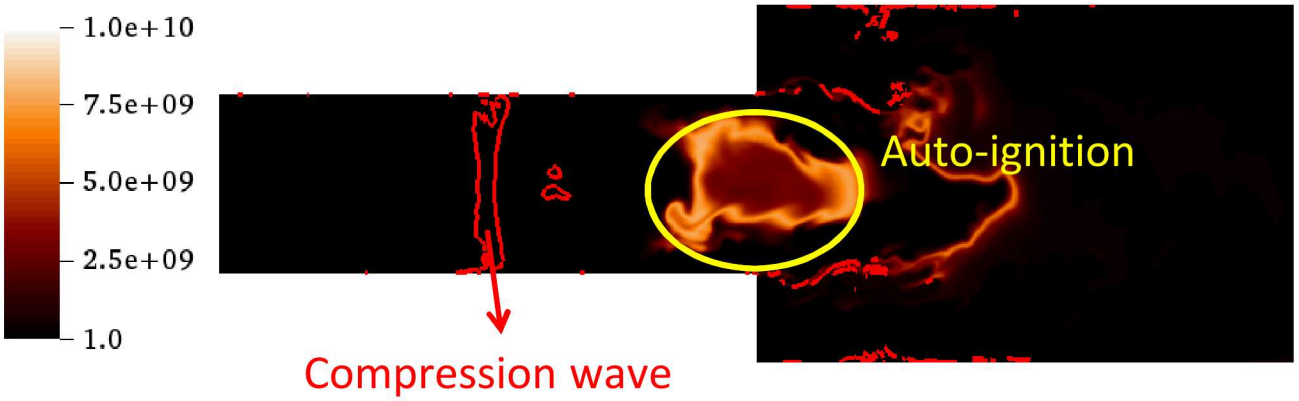

Contours of heat release

Compression wave

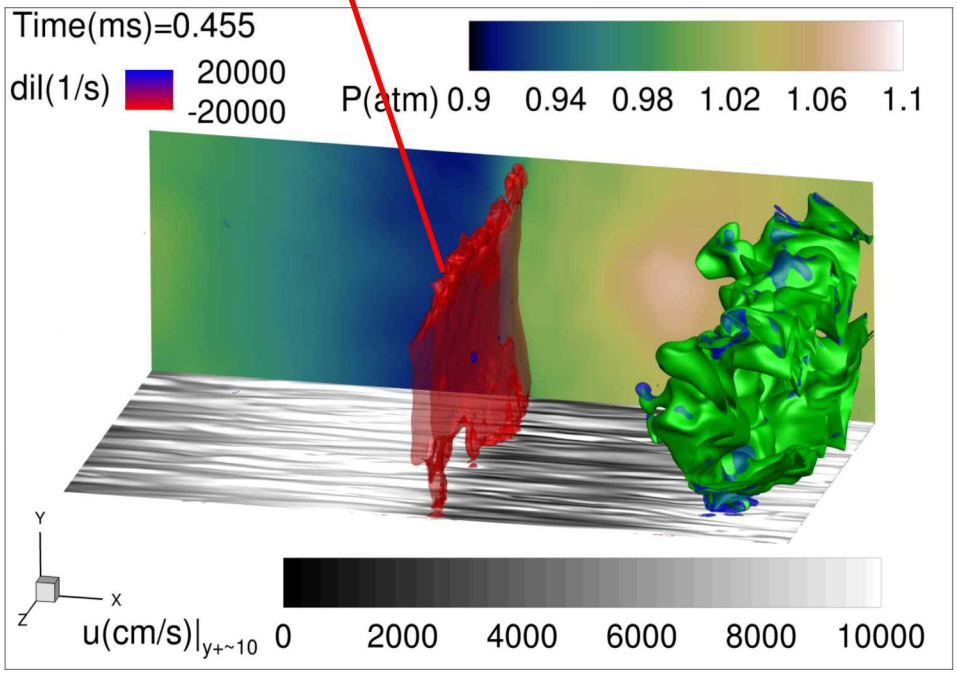

- Local rise in pressure
- Increases local temperature by 20-30 K
- High reactivity of hydrogen
- Decrease in ignition delay time (30%)

Conclusions

- Performed DNS of a reheat burner at scaled conditions
- Two states of hydrogen/air combustion have been observed:
  - design state: flame propagation and auto-ignition in the combustor
  - intermittent auto-ignition in mixing section
- Premature auto-ignition arises due to pressure (and following temperature) rise in mixing section
- Quantified the contribution of different modes towards heat release using chemically explosive mode analysis (CEMA)
- Future work:
  - characterize the unstable flame behavior and the conditions leading to it
  - find the inlet conditions for statistically stationary reheat flame
  - perform 2D and 3D simulations with varying fuel composition and its stratification

ECP has formulated a holistic approach that uses co-design and integration to achieve capable exascale

Application Development	Software Technology	Hardware Technology	Exascale Systems
Science and mission applications	Scalable and productive software stack	Hardware technology elements	Integrated exascale supercomputers

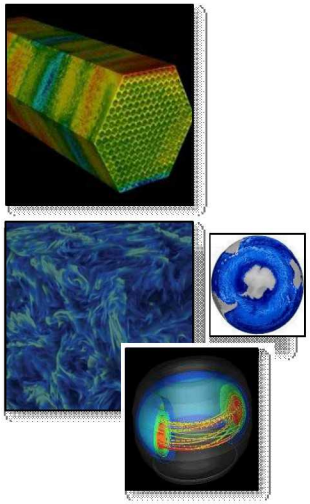

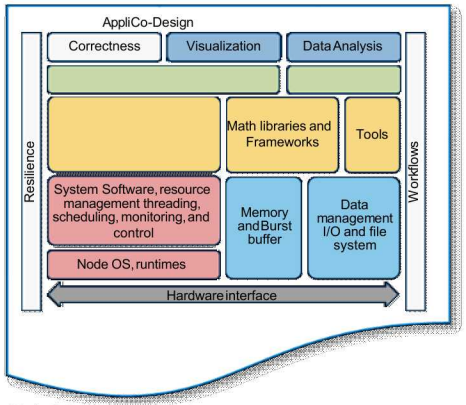

ECP's work encompasses applications, system software, hardware technologies and architectures, and workforce development

From Paul Messina's ASCAC talk April 19, 2017

ECP application: Transforming Combustion Science and Technology Through Exascale Simulation (Pele)

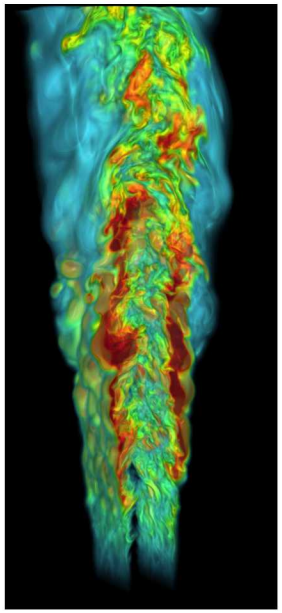

S3D: multi-block compressible reacting DNS multi-physics validation: spray, soot, radiation

Effects of reactivity stratification at:

- high pressure
- high turbulence
- fuel blends

on:

- ignition delay
- combustion rates
- emissions

Pele: Block-structured adaptive mesh refinement, multi-physics: spray, soot, and radiation, real gas, complex geometry

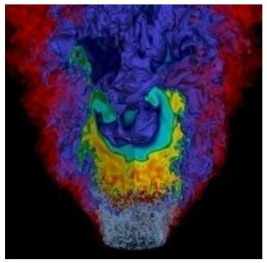

Automated Mechanism Generation

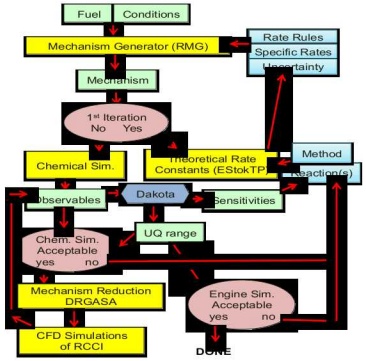

The Pele Project

Transforming Combustion Science and Technology with Exascale Simulations

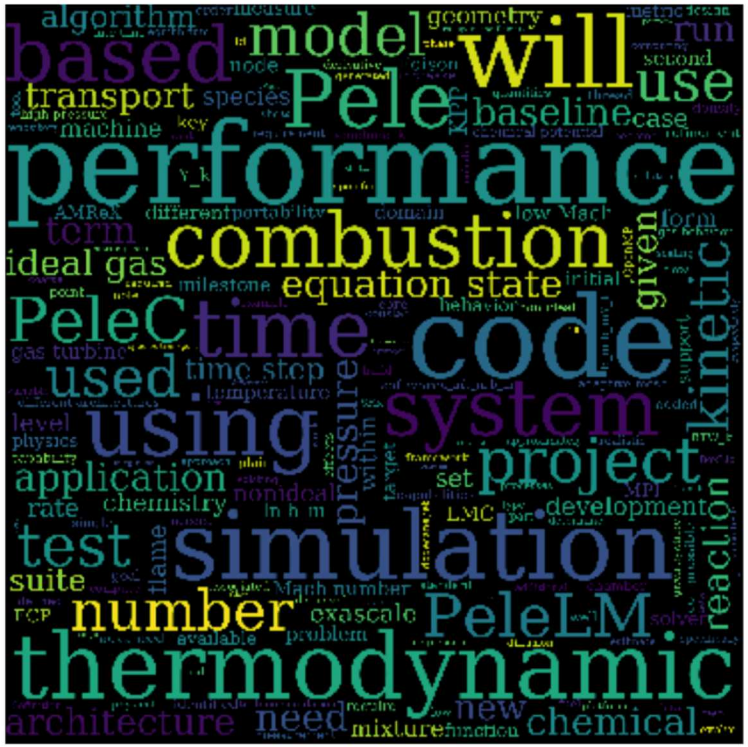

- Use exascale platforms to solve first of exascale-era combustion problems
- Anchored in basic research needs: requirements driven by gas phase chemical kinetics research questions

  - turbulence chemistry interaction in conditions *motivated by IC engine research*
  - provide a path for development of scalable design codes suitable for exascale hardware

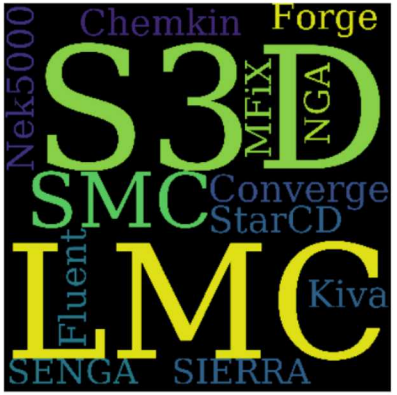

Challenge Problem - Motivation

Advanced combustion regimes (LTC)

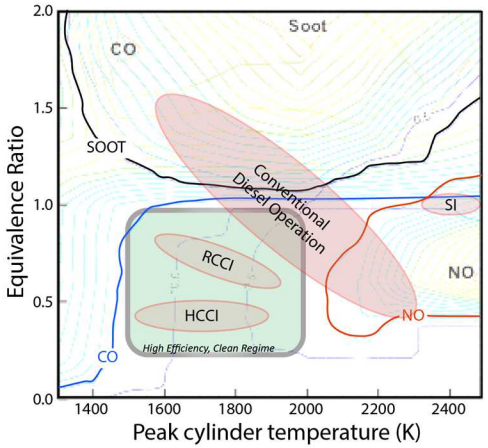

Conventional diesel *

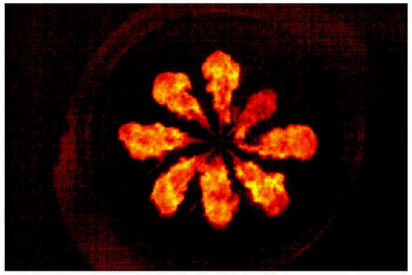

Early injection PCCI

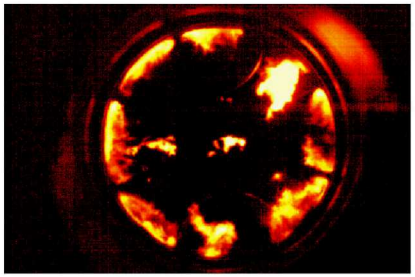

PCCI/HCCI – load limitations
Requires precise charge preparation and combustion control mechanisms
(for auto-ignition and combustion timing)

Adapted from content provided by University of Wisconsin Engine Research Center

High Fidelity DNS and Hybrid DNS/LES of RCCI Diesel Combustion

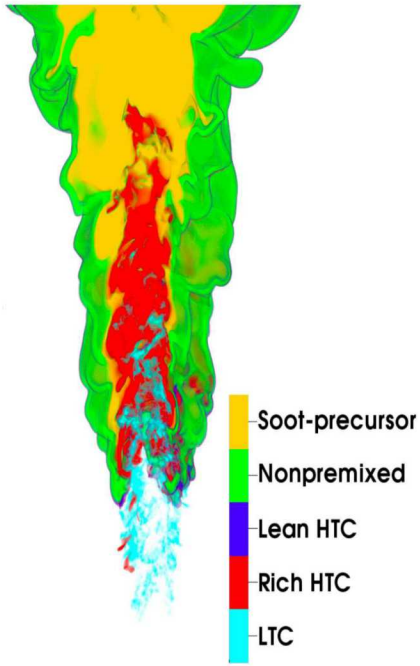

DNS of a ndodecane spatially evolving turbulent diesel jet flame at 60 bar, combustion modes, Dalakoti et al. 2018

Characteristic / Need	Approach
Impulsively started jets with disparate scales between fronts and turbulence. (Outer scales: 10cm, ms Inner timescales: microns, ns)	Dynamic adaptive mesh refinement
High speed injection followed by subsonic conditions downstream	Compressible and low-Mach capabilities
Long time horizons to set up turbulence for studying fundamental TCI	Hybrid DNS/LES [Non-reacting LES, DNS for flame]
Lean, rich, and low temperature chemistry critical in multi-stage ignition and formation of soot precursors.	Accurate and detailed thermochemistry.
Liquid fuel injection	Lagrangian spray model
Coupling between mixture preparation and emissions	Detailed kinetics including emissions, sectional model for soot with radiation
Mixture preparation dependent on re-entrainment of combustion products	Realistic piston dish and cylinder wall geometry
Performant on exascale architecture	

Design Philosophy, Strategy

- The Pele suite:
  - Compressible (**PeleC**) and low Mach number (**PeleLM**) integrators, compatible design, data, I/O, etc
  - Shared physics (ideal/real gas kinetics, thermodynamics, transport, sprays, etc) - **PelePhysics**
  - Block-structured adaptive mesh refinement, built on **AMReX** framework
  - Robust, accurate, extensible finite-volume (conservative) discretizations
  - Embedded boundary treatment of arbitrary geometries
    - Enables CAD-to-compute, avoids expensive, time-consuming difficult mesh generation step
  - AMReX-supported X+Y parallelism (inter-node X and intra-node Y)
  - Parallel mesh and particle data, specialized to needs of AMR (temporal subcycling, etc), plus Fork-Join type temporary redistribution strategies, high-performance I/O and in-situ/in-transit analysis support
  - Combustion-specific agile code generation: Fuego+SINGE for GPU-optimized CUDA kinetics evaluation, Kokkos-based kernels for particle/fluid coupling terms
- Agile development framework, open source modular design, continuous integration/testing
- Close interaction with AMReX for new capabilities in development
  - App-relevant GPU/A21 implementation of AMReX structures/algorithms
  - Leverage AMReX multi-app development

Pele Code Design Overview

- Baseline algorithm design for multicomponent flow with stiff reactions, AMR
  - **PeleC**: Comparable advection, diffusion time scales, motivates IMEX-type scheme based on Spectral Deferred Corrections (**SDC**) with *time-implicit* chemistry
    - Robust highly efficient time-explicit Godunov-type upwind advection, simple centered diffusion
    - BDF-style implicit chemistry ODE integration, with sources that approximate the other processes
  - **PeleLM**: acoustics filtered away analytically, but still want robust, time-explicit advection
    - Chemistry *and* diffusion are now *time-implicit* – ***iterative timestep*** simultaneously incorporates flow constraint (constant pressure), mutually coupled species/energy diffusion and chemistry. Entire system evolved stably on slower advection time scales across AMR grid hierarchy
- SDC-based iterative timestep – treats each process essentially independently, with accelerated iteration to couple everything nicely together
- Robust baseline allows stable, well-behaved *extensible* time step
  - Switch 2^{nd} order advection scheme with more accurate 4^{th} order algorithm
  - Option for “destiffened” chemistry model that allows highly efficient time-explicit advance
  - Robust to other, potentially stiff, tightly coupled processes, such as sprays, radiation, soot, etc

Project Roadmap

	2017	2018	2019	2020	2021	2022
Model Development	**Hybrid LES/DNS** ✓	**Deep learning SGS model training methodology**	**Rare event detection**		**In situ training**	
Compressible Capabilities	Non-ideal, ✓ single level sprays, ✓ static EB geometry ✓	Non-reacting LES, ✓ AMR sprays ✓	Hybrid LES/DNS	Soot	Radiation	Moving EB geometry
Capability Towards Challenge Problem	 **60 Bar open, gas phase dodecane low mach jet**	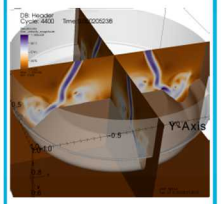 **Atmospheric pressure, compressible static geometry flows**	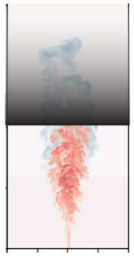 **60 Bar open, ideal gas dodecane low mach jet wall impingement**	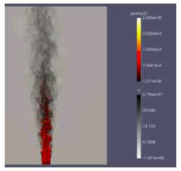 **60 Bar open, dodecane jet with hybrid multi-physics**	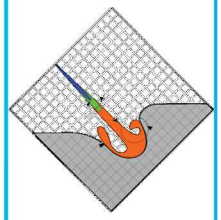 **60 Bar compressible + low Mach, re-entrainment**	
Low Mach Capabilities			Static EB geometry	Sprays, Hybrid LES/DNS	Hybrid compressible / LM Non-ideal EOS	
Automated Thermochem	**Initial demonstration** ✓	**Pressure independent kinetics**	**Mechanism generation**	**Reduced dual-fuel mechanism**		
Performance and software	PeleC Exists ✓ Understand potential of task parallel ✓	PeleLM tiling	GPU performance Multi-physics load balancing	Performance portability		A21 / Frontier Performance Enhancements

DNS of Multi-Injection Diesel Combustion with PeleLM

M. Rieth[1], M.S. Day[2] and J. H. Chen[1]

[1]Sandia National Laboratories
[2]Lawrence Berkeley Laboratories

Office of Science
U.S. Department of Energy

EXASCALE COMPUTING PROJECT

DNS of Ndodecane Multi-injection Jet at Diesel Conditions - Parameters

- N-dodecane/air injection with $Y_{NC12H26}$ =0.45, 446K
- Jet: D=0.17mm, U=30m/s, Re=15,000
- Environment: 60 bar, 900K, 15/85% O2/N2 (‘spray A’)
- 10 micron resolution
- 53 species mechanism
- Age variable tracks the fluid age/residence time

Diffusion coefficient based on Le=1 for all add. scalars

$$\frac{\partial \rho a}{\partial t} + \frac{\partial \rho u_j a}{\partial x_j} = \frac{\partial}{\partial x_j}\left(\rho D \frac{\partial a}{\partial x_j}\right) + \rho$$

40

Reactor studies – standard conditions ('spray A')

Fuel side: NC12H26/air @Z=0.45 & 446K, oxidizer: 15%O2 900K, 60atm

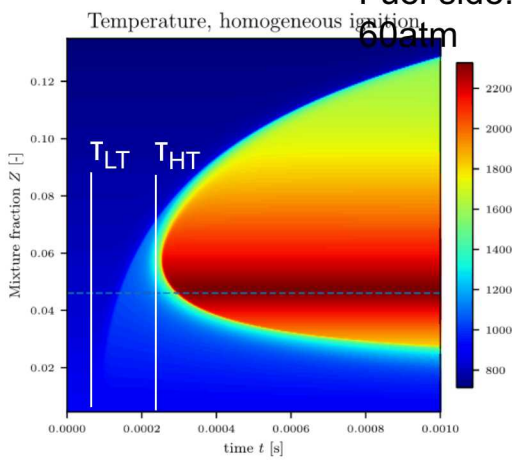

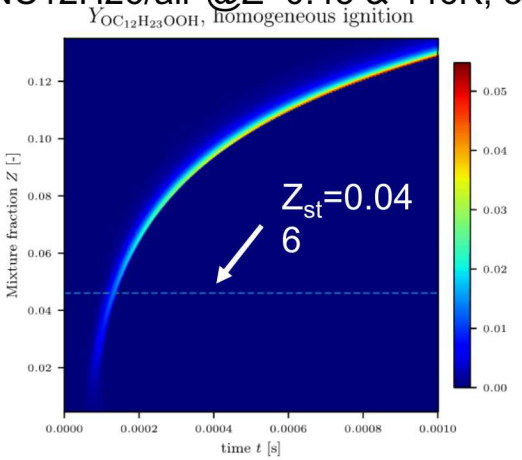

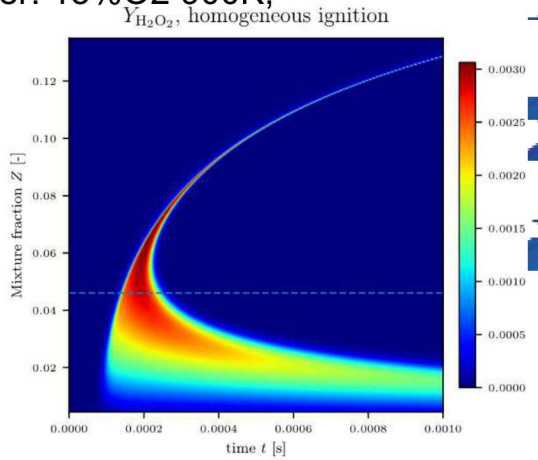

Low T ign.: 0.05ms, Z<0.02

High T ign.: 0.25ms, Z=0.057 (~1.24 Z_{st})

$\Delta\tau_{HT,LT}$=0.2ms

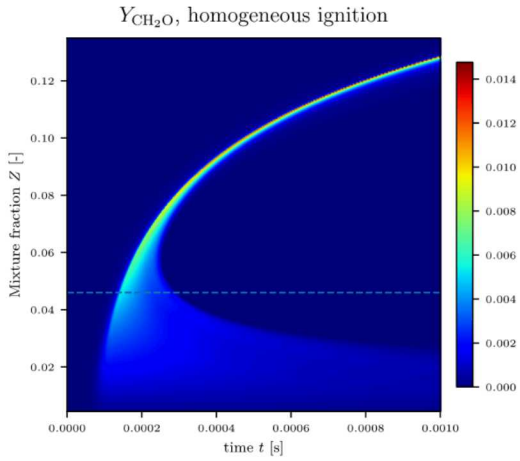

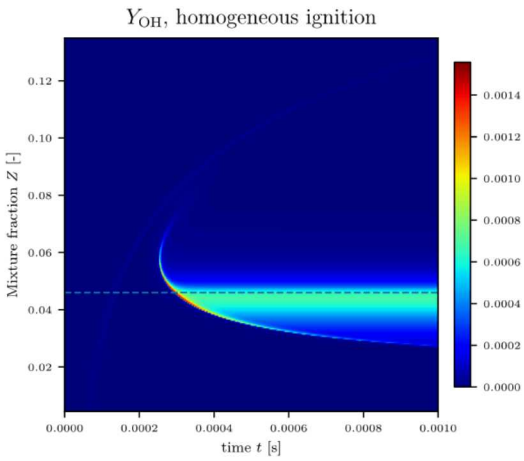

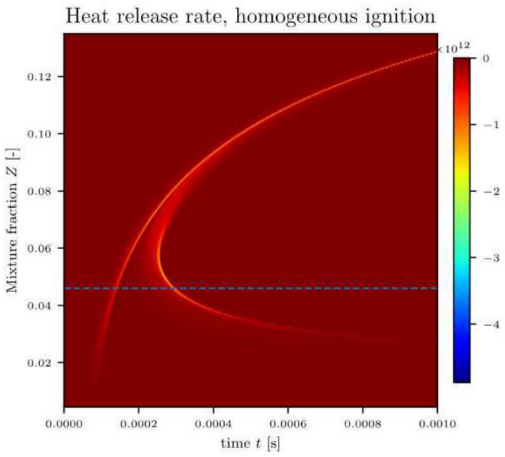

41

Reactor studies – oxidizer consists of lean products (Z=0.025)

Fuel side: NC12H26/air @Z=0.45, oxidizer: equilibrated NC12H26/air @Z=0.025, 60atm

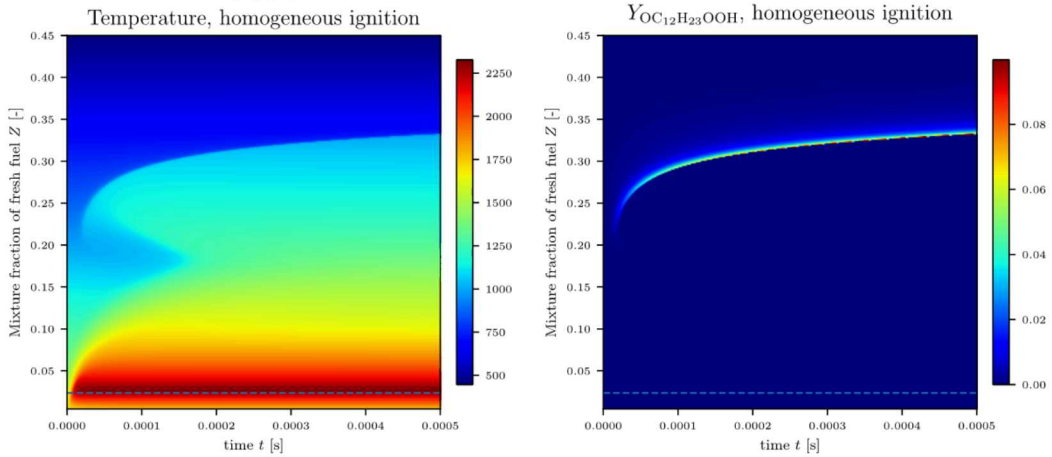

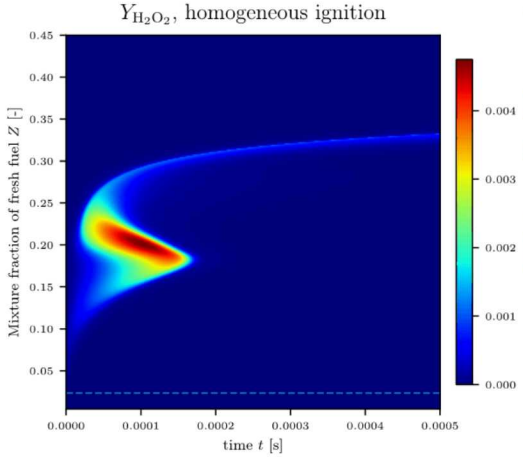

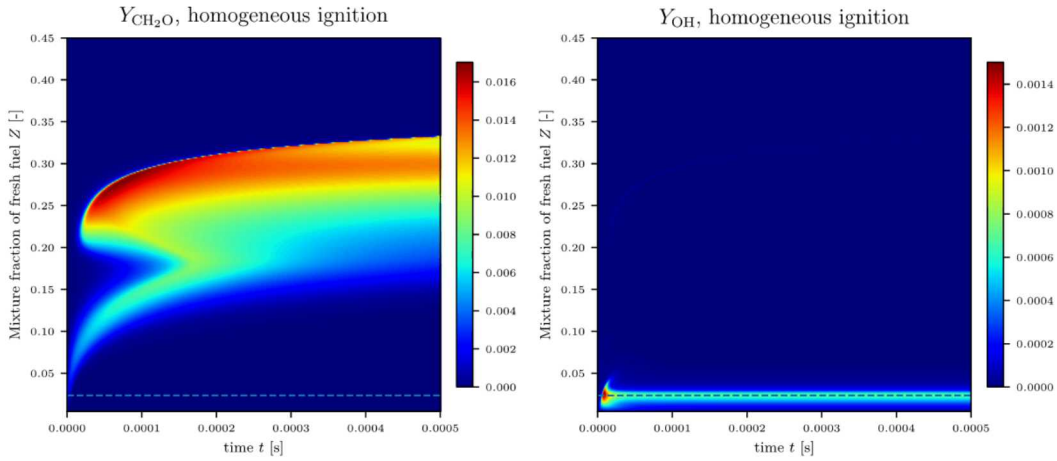

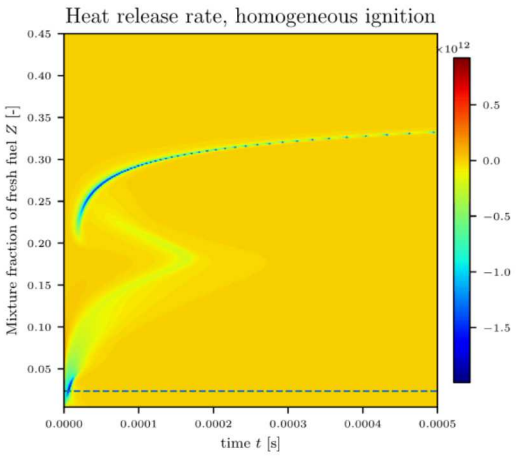

Low T ign.: 0.03ms, Z=0.2

High T ign.: <0.01ms, Z<0.02 (<~0.44 Z_{st})

$\Delta\tau_{HT,LT}$ < 0 ms

42

EXASCALE COMPUTING PROJECT

Reactor studies – oxidizer consists of lean products (Z=0.01)

Fuel side: NC12H26/air @Z=0.45, oxidizer: equilibrated NC12H26/air @Z=0.01, 60atm

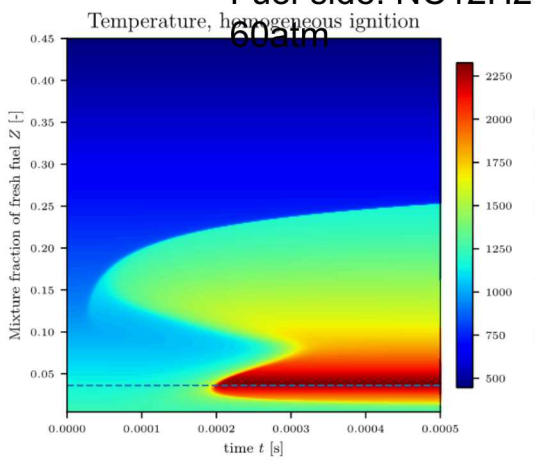

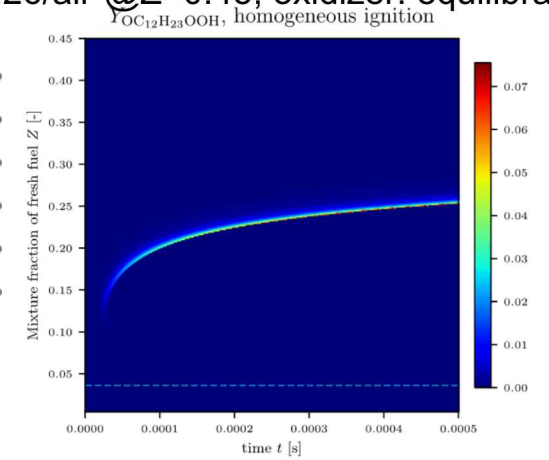

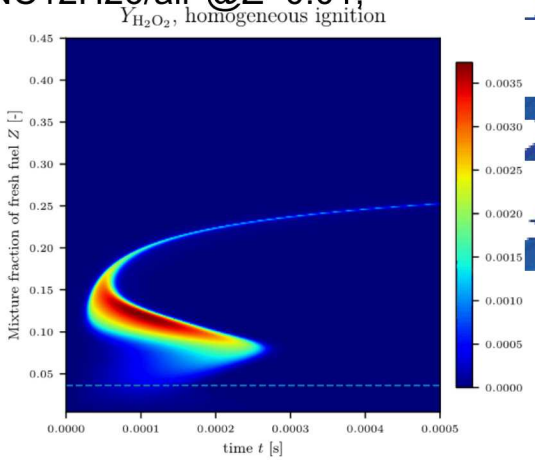

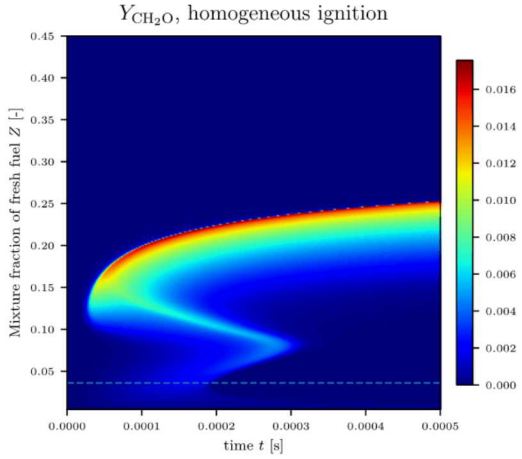

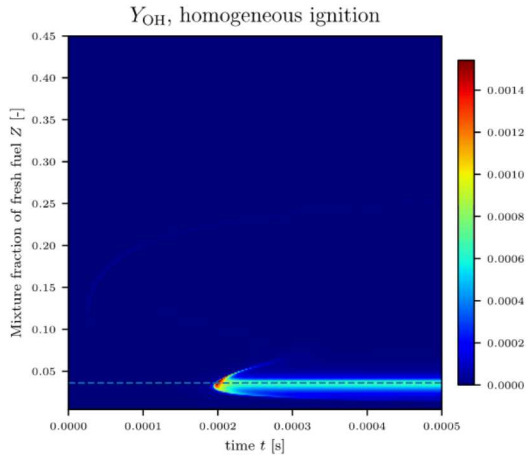

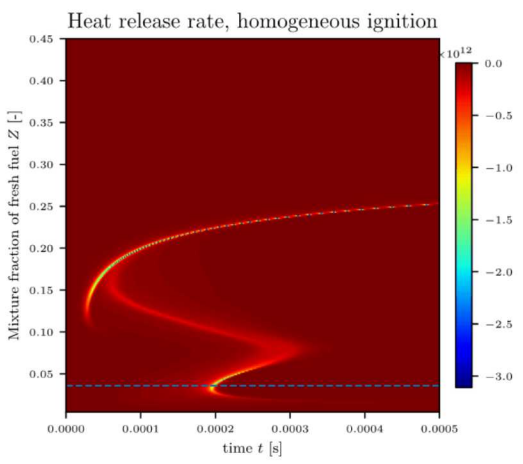

Low T ign.: 0.05ms, Z=0.12

High T ign.: 0.2ms, Z=0.042 (~0.91 Z_{st})

$\Delta\tau_{HT,LT}$=0.15ms

43

Comparison at 0.4ms after pilot/main injection start

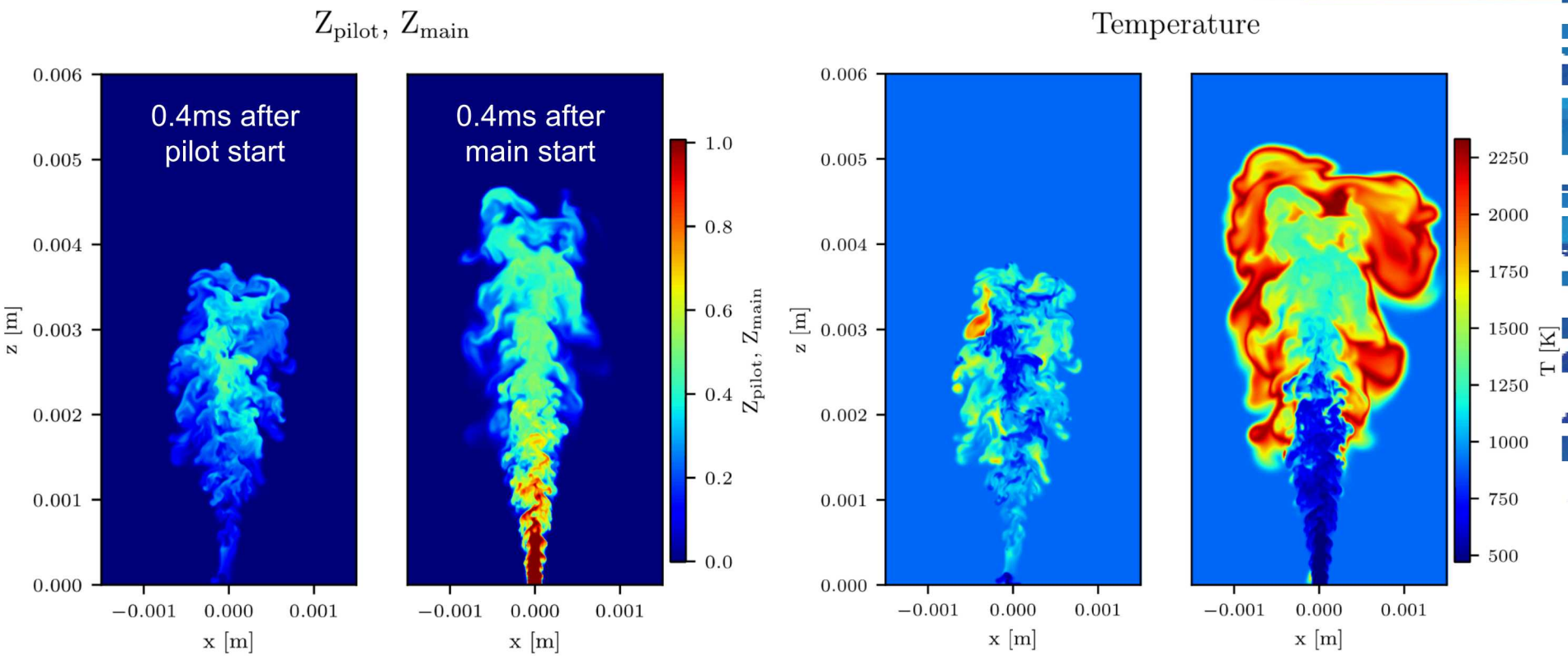

Pilot: 0.26ms, dwell: 0.17ms, main: 0.74ms
left: times w.r.t pilot start (0.4ms total time), right: times w.r.t. main start (0.83ms total time)

44

Comparison at 0.4ms after pilot/main injection start

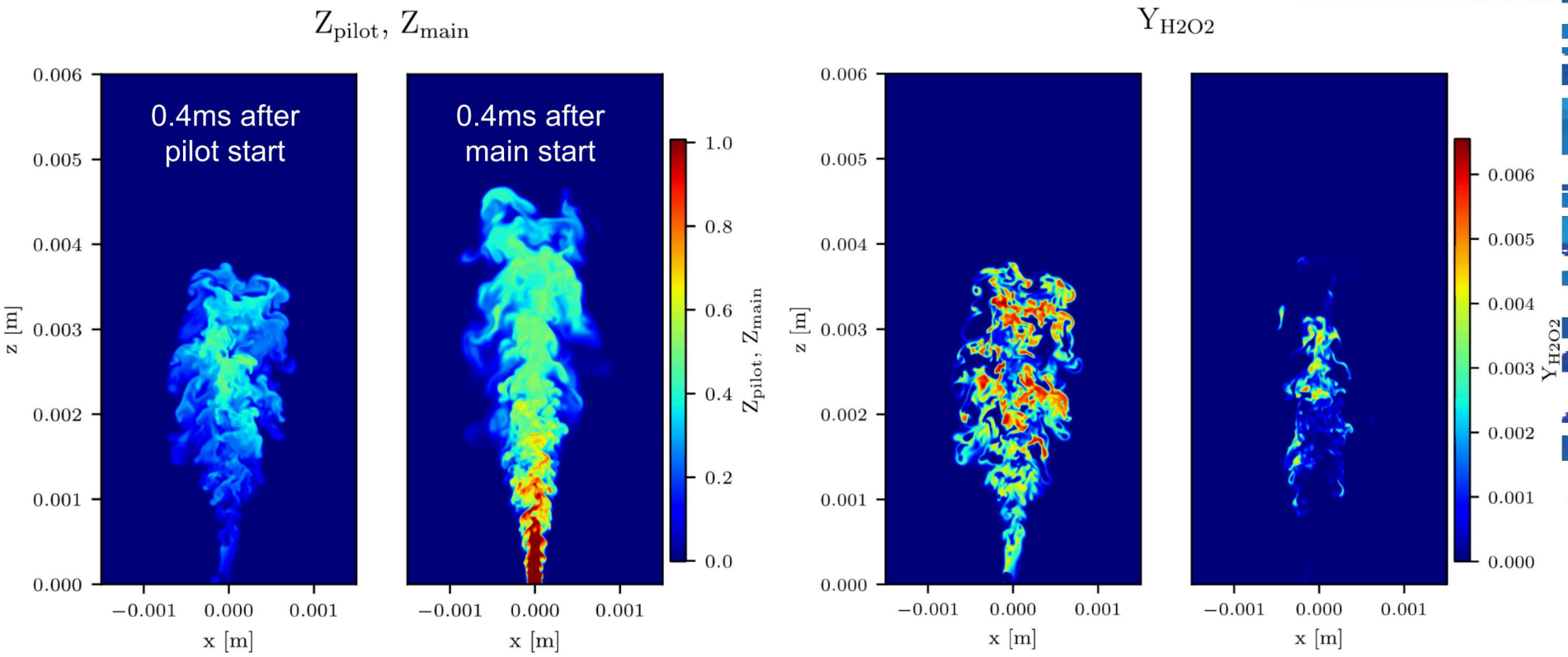

45

Comparison at 0.4ms after pilot/main injection start

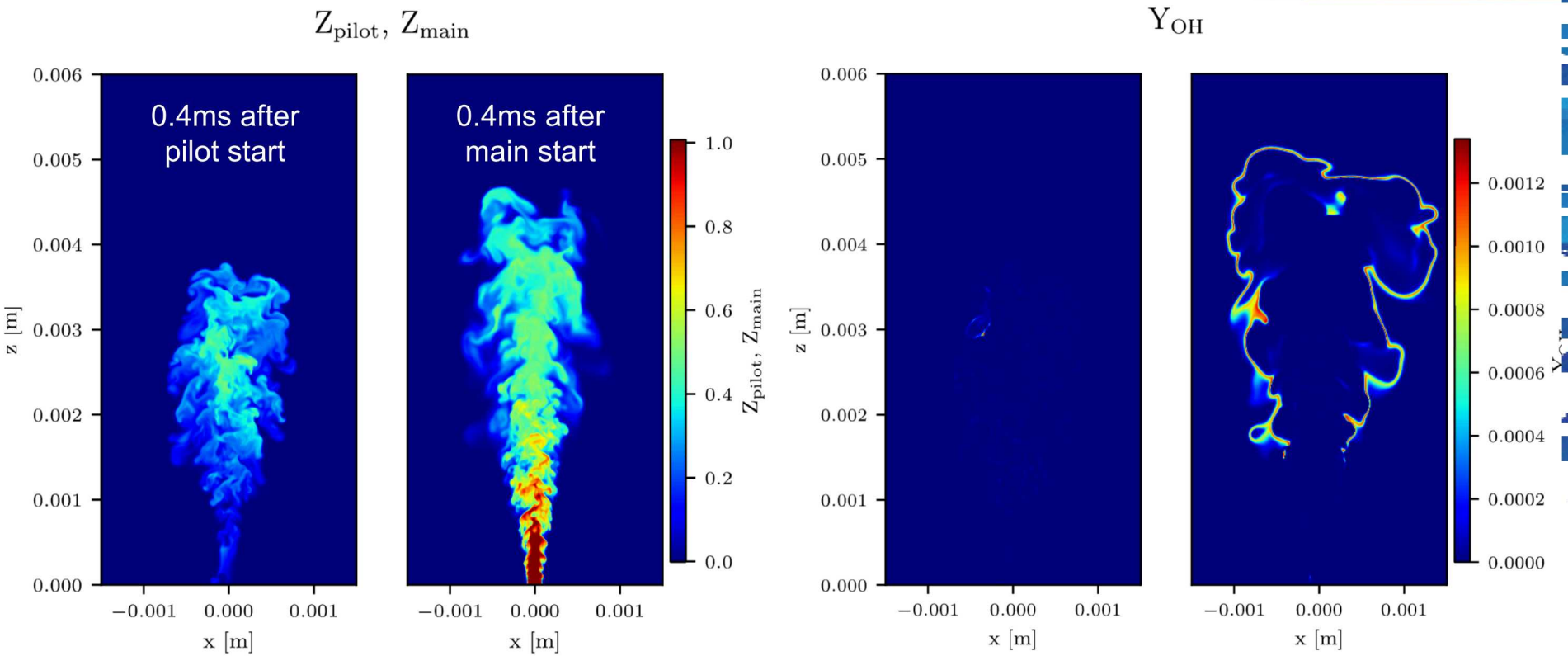

46

Comparison at 0.4ms after pilot/main injection start

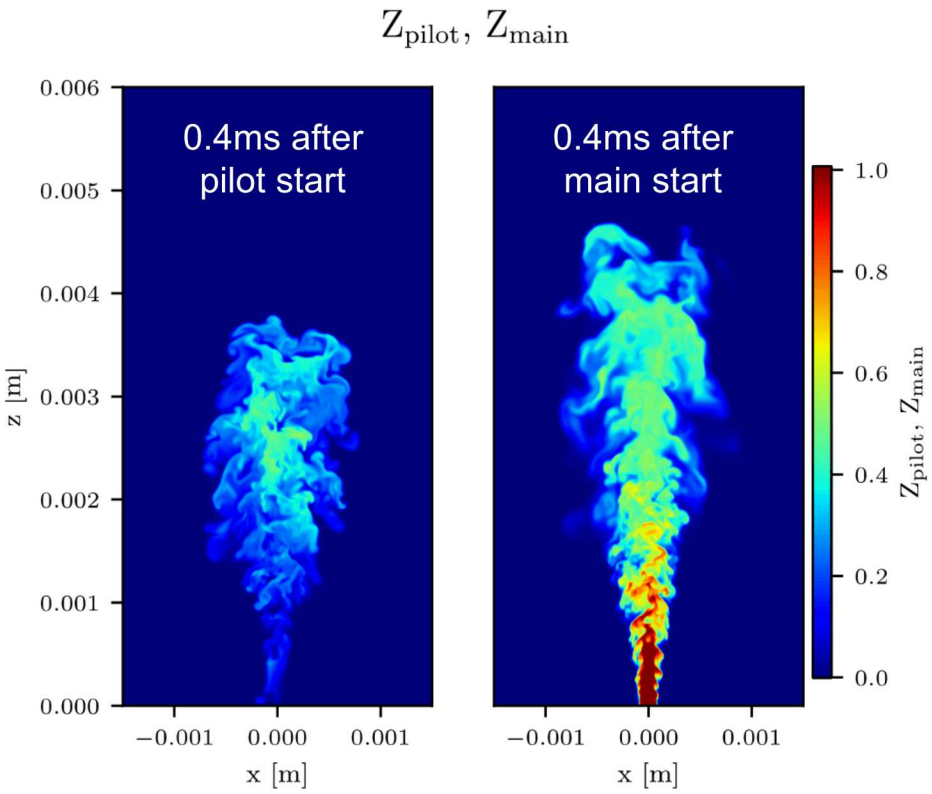

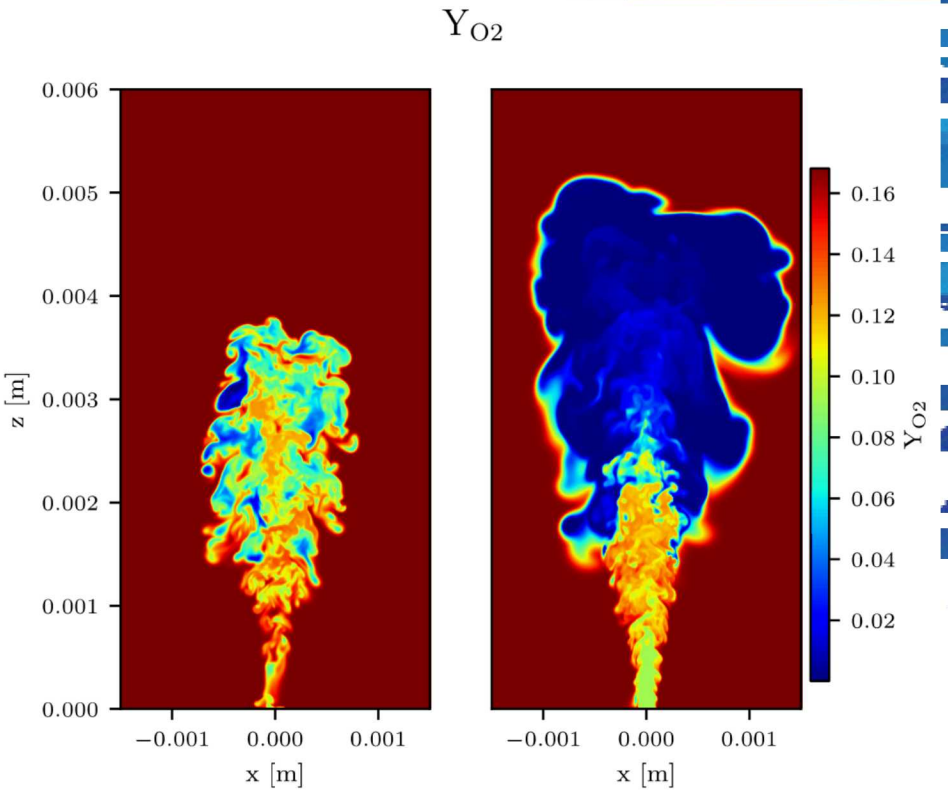

47

Comparison at 0.4ms after pilot/main injection start

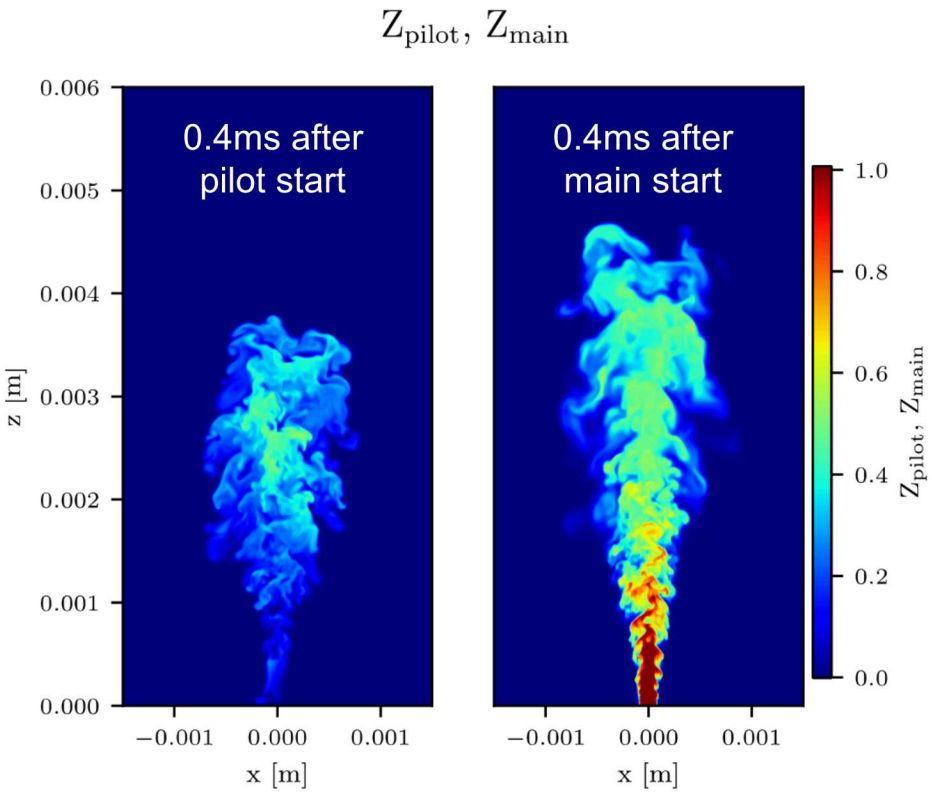

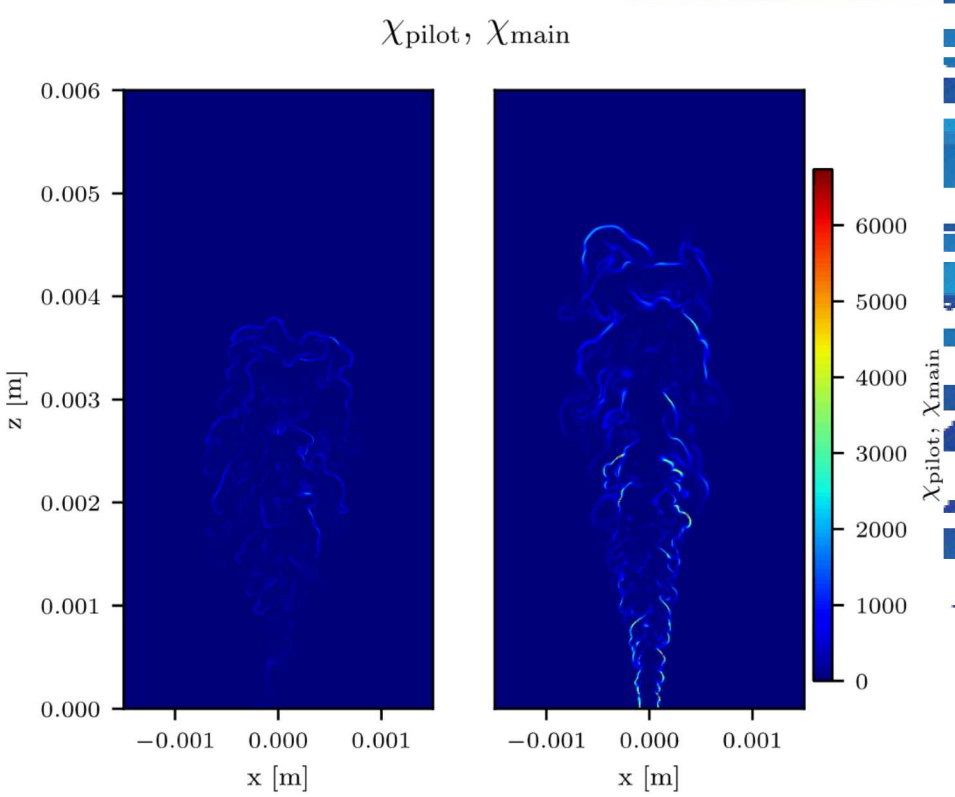

48

Difference in pilot and main ignition - temperature

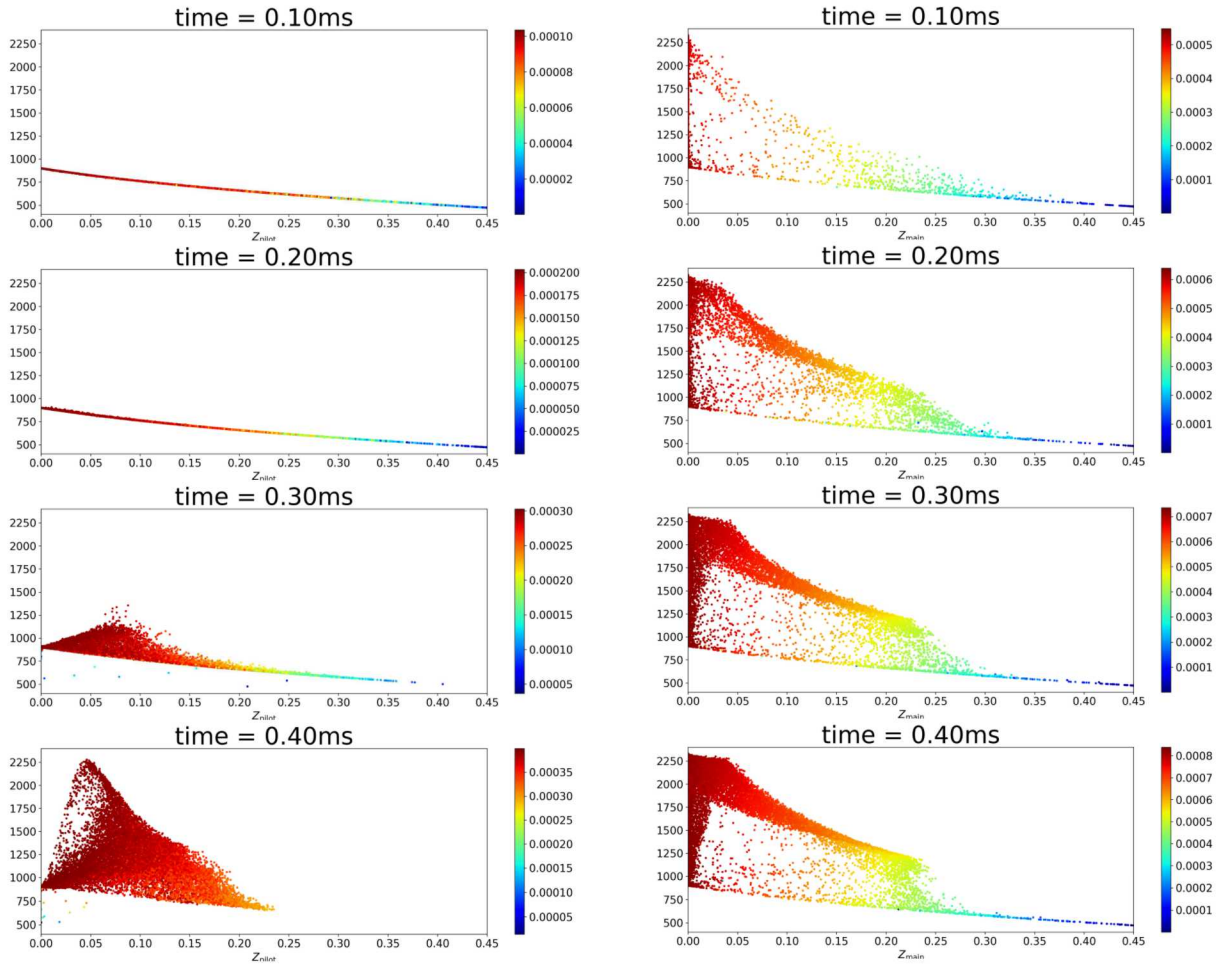

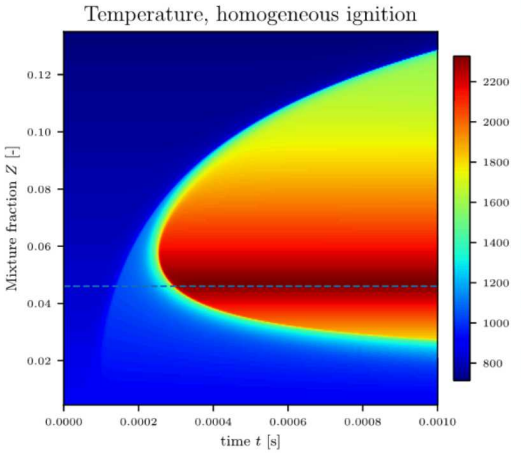

Pilot:
-Stoich. conditions close to homogeneous ign.
-Difference for rich cond.

Main:
-Significant differences on rich side

Pilot: 0.26ms, dwell: 0.17ms, main: 0.74ms; left: times w.r.t pilot start, right: times w.r.t. main start

49

Difference in pilot and main ignition – OC12H23OOH

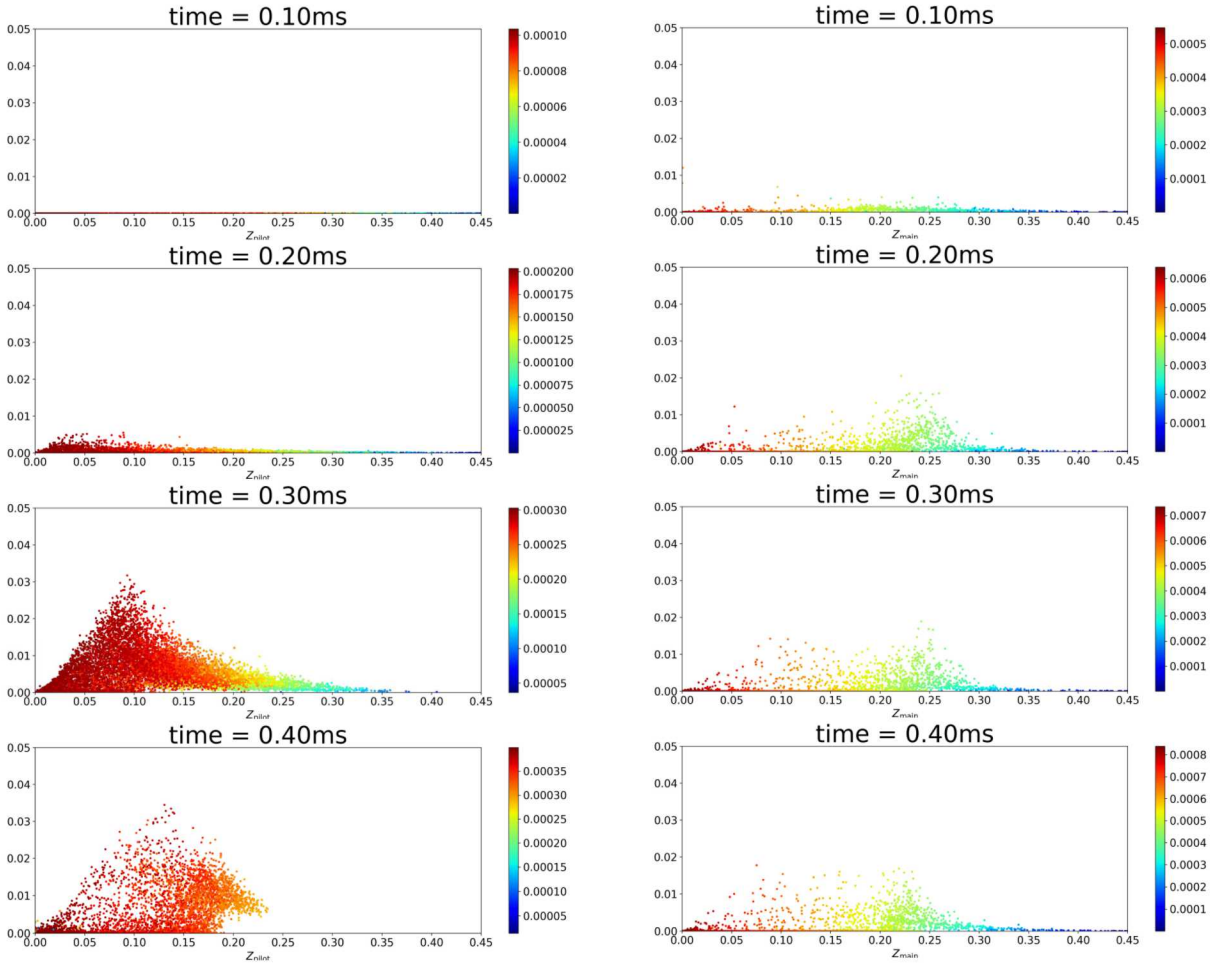

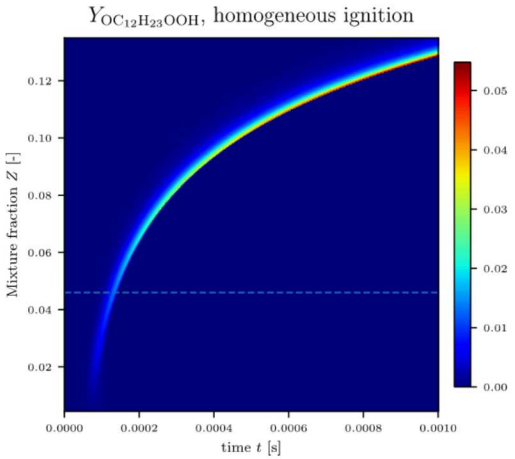

Pilot: 0.26ms, dwell: 0.17ms, main: 0.74ms; left: times w.r.t pilot start, right: times w.r.t. main start

50

Difference in pilot and main ignition – H2O2

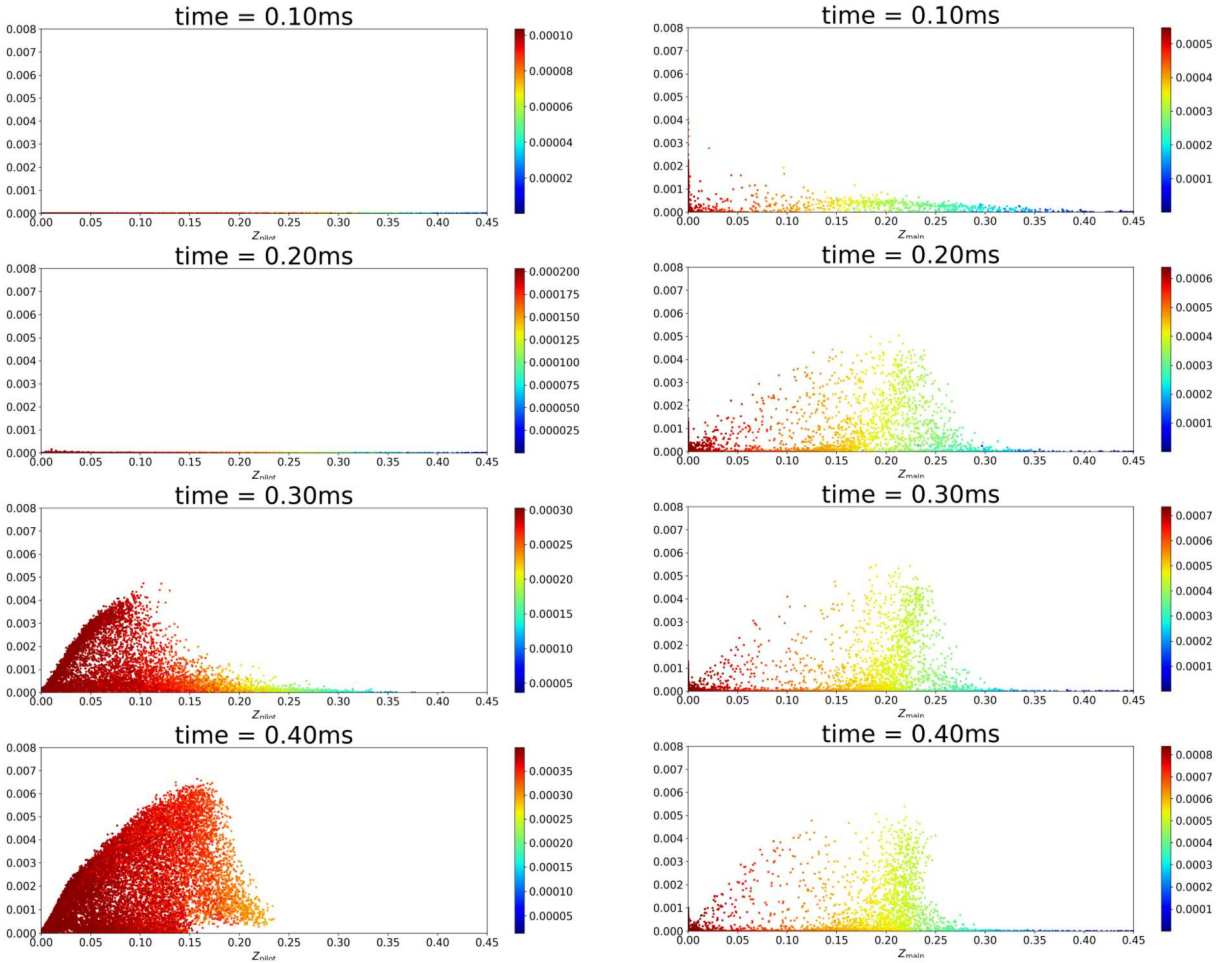

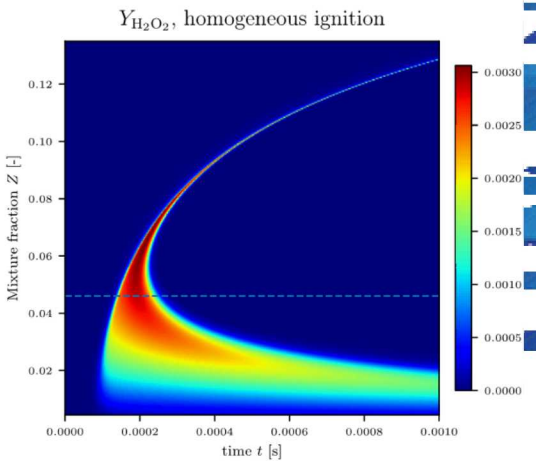

Pilot: 0.26ms, dwell: 0.17ms, main: 0.74ms; left: times w.r.t pilot start, right: times w.r.t. main start

51

Combustion simulations

Iso-surfaces of vorticity magnitude colored by temperature

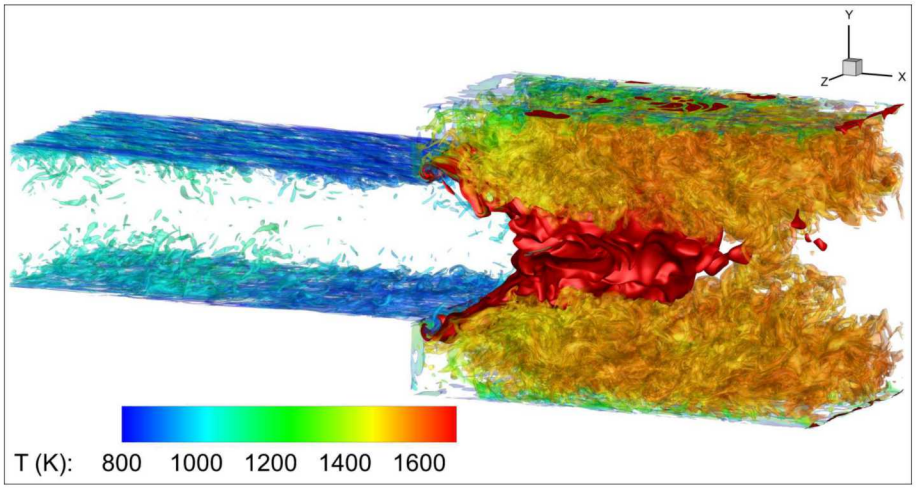

- Multi-variate data: ~10 – 100 variables
- Direct numerical simulations: resolve all the scales in space and time
- Massively parallel solvers (e.g. S3D Chen at al. (CSD 2009))
  - computationally expensive (tens millions of CPU hours)
  - large amount of data (~ 100 TB)
- Exascale (millions processing elements): need efficient workflows

Simulation workflow

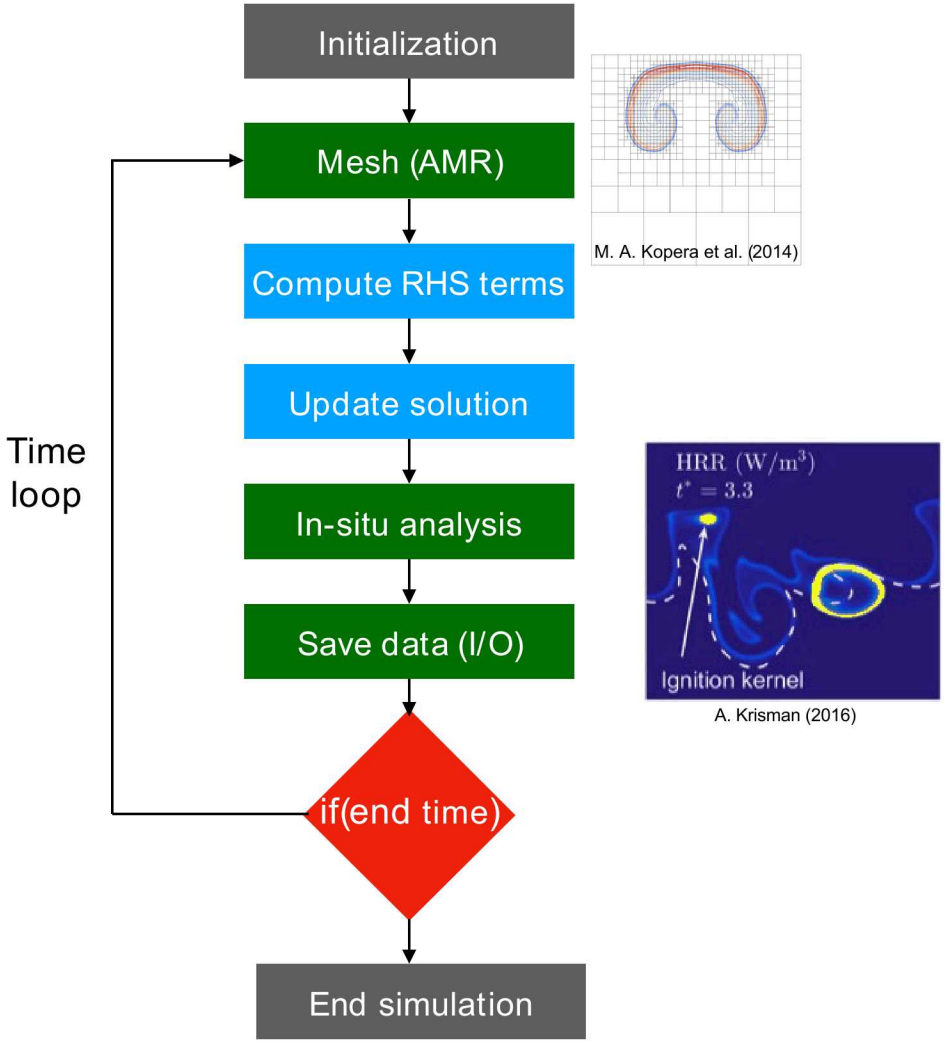

Results

- k-nearest neighbors
  - compute “mean” distance from k nearest neighbors
- Local outlier factor
  - compute outlier score based on local density
- Supervised learning methods (e.g. neural networks)
  - regression and classification

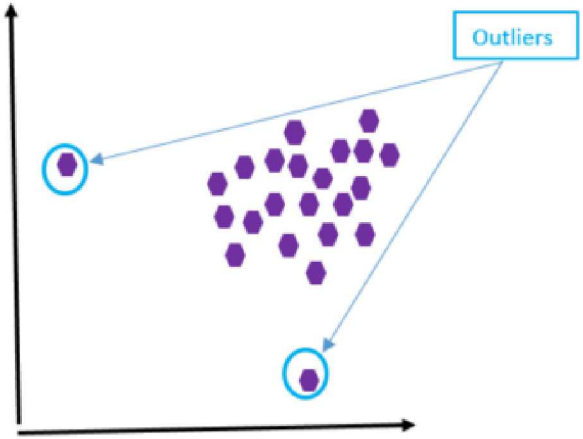

Not efficient and expensive to compute

Idea

- Bivariate dataset

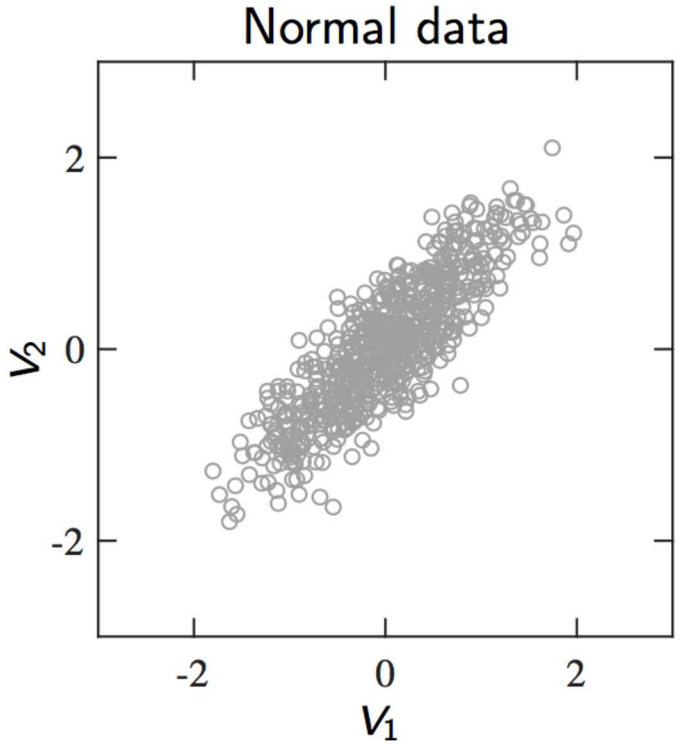

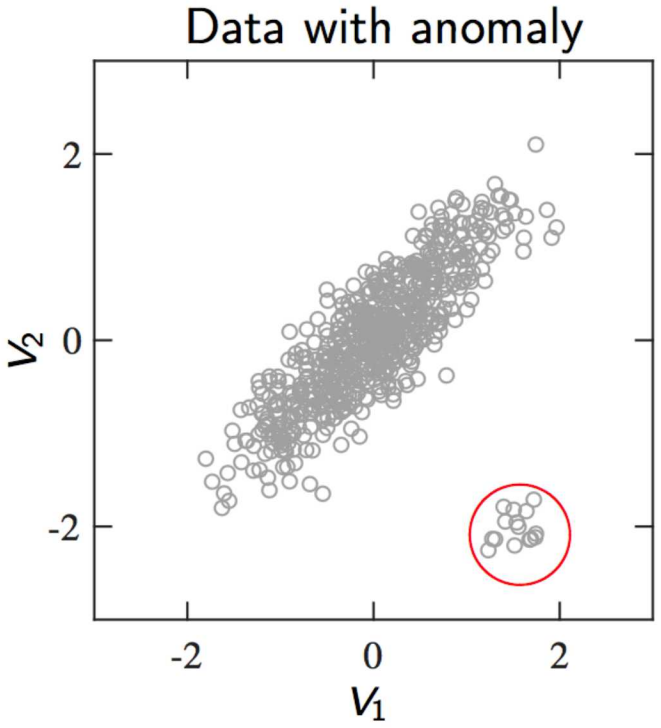

- Characterize the data distribution: principal component analysis
- Change in distribution: effects the magnitude of principal value and orientation of principal vectors

Principal component analysis

- Scale the data: with mean and maximum
- Compute the co-variance matrix (second order joint moment)
- Perform Eigen decomposition to obtain the principal values and vectors

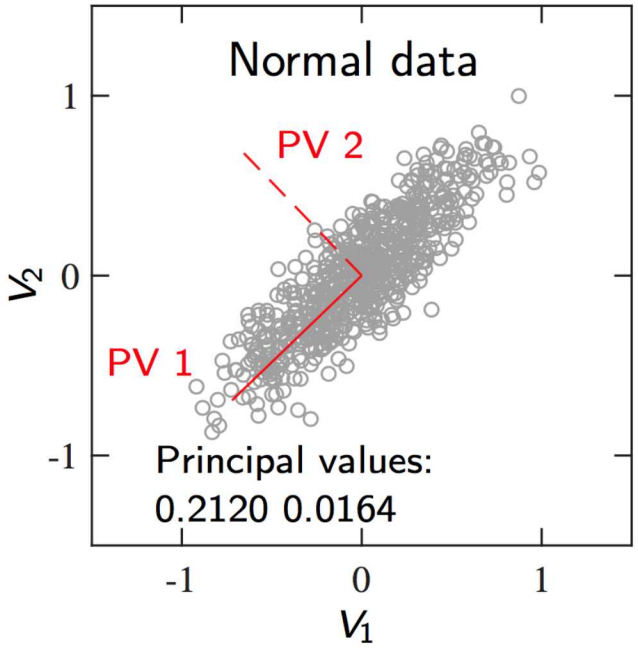

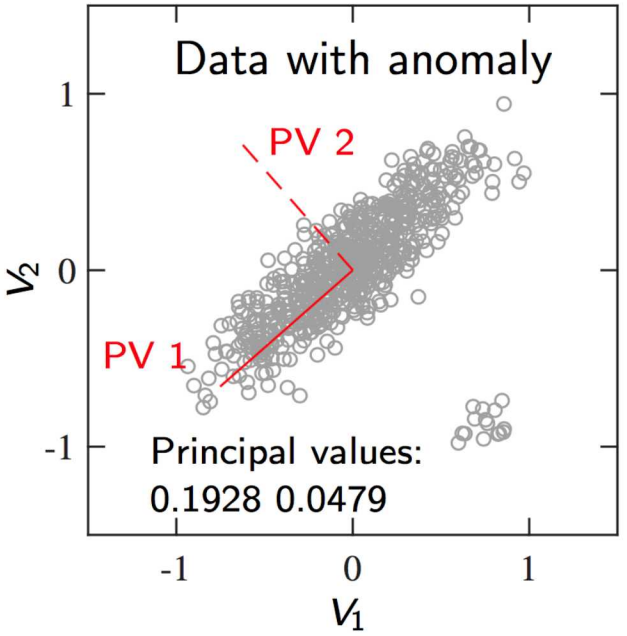

- Mainly captures variance
- **Need to look at higher order moments to capture extreme events**

Fourth order joint moment

Kurtosis: measure of "either existing outliers (for the sample kurtosis) or propensity to produce outliers (for the kurtosis of a probability distribution)" (P. H. Westfall, 2014)

- Compute the fourth joint moment (cumulant tensor, T)

$$\begin{aligned}\mathcal{T} \;=\; & \mathbb{E}[v \otimes v \otimes v \otimes v] - \mathbb{E}[v_{i_1} v_{i_2}]\mathbb{E}[v_{i_3} v_{i_4}] \\ & -\mathbb{E}[v_{i_1} v_{i_3}]\mathbb{E}[v_{i_2} v_{i_4}] - \mathbb{E}[v_{i_1} v_{i_4}]\mathbb{E}[v_{i_2} v_{i_3}], \quad 1 \leq i_1 \ldots i_4 \leq k\end{aligned}$$

- Decompose the fourth order symmetric tensor
  - Tensor size (N_f^4), N_f : number of features
  - Matricize the tensor and perform SVD (A. Anandkumar et al., JMLR 2014)
- Obtain principal kurtosis values and vectors

Anomaly detection

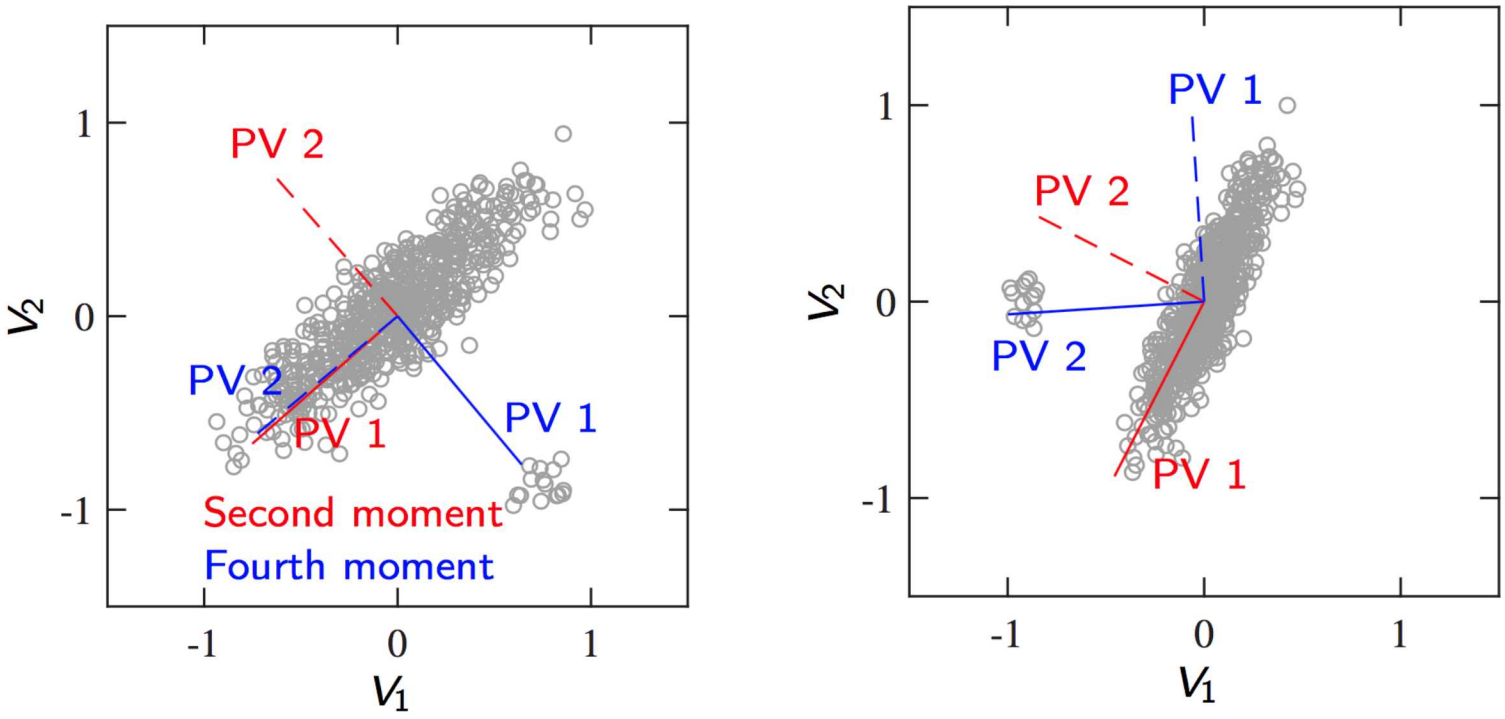

- First principal kurtosis vector aligns in the direction of anomalies
- Can be used to characterize extreme events

Results

Consider a simple problem with a 1D domain

- Initial condition

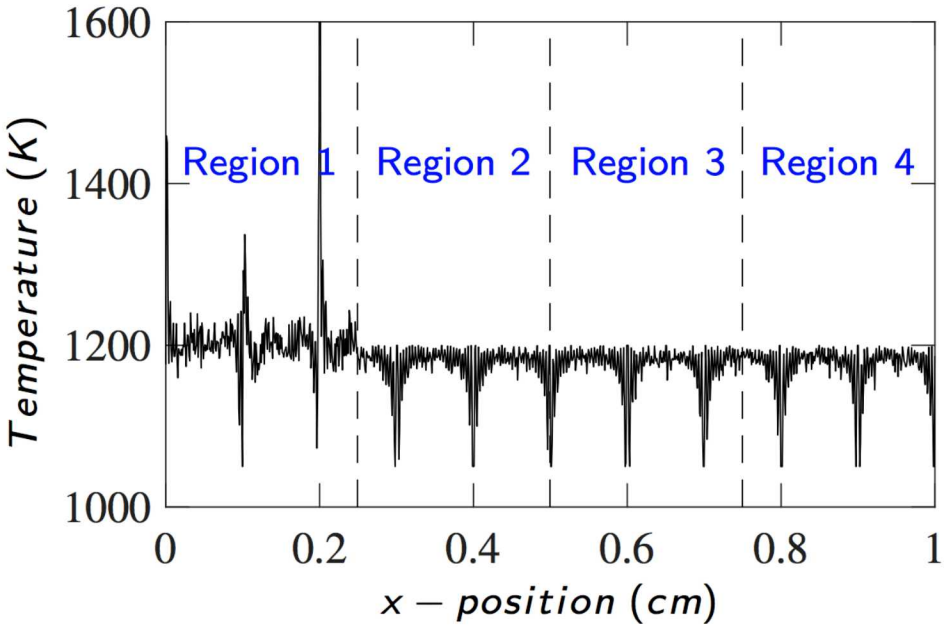

- Fuel-air composition: premixed – $0.6CO + 0.4H_2 + 0.5(O_2 + 3.76N_2)$
- Solver: scalable reacting flow code S3D (J. H. Chen et al., CSD 2009)
- Number of subdomains: $N_d = 4$
- Time-steps: $\Delta t = 0.001\ \mu s$
- Number of checkpoints: $N_t = 20$, interval: 1 μs

Auto-ignition test case

- Time evolution of temperature

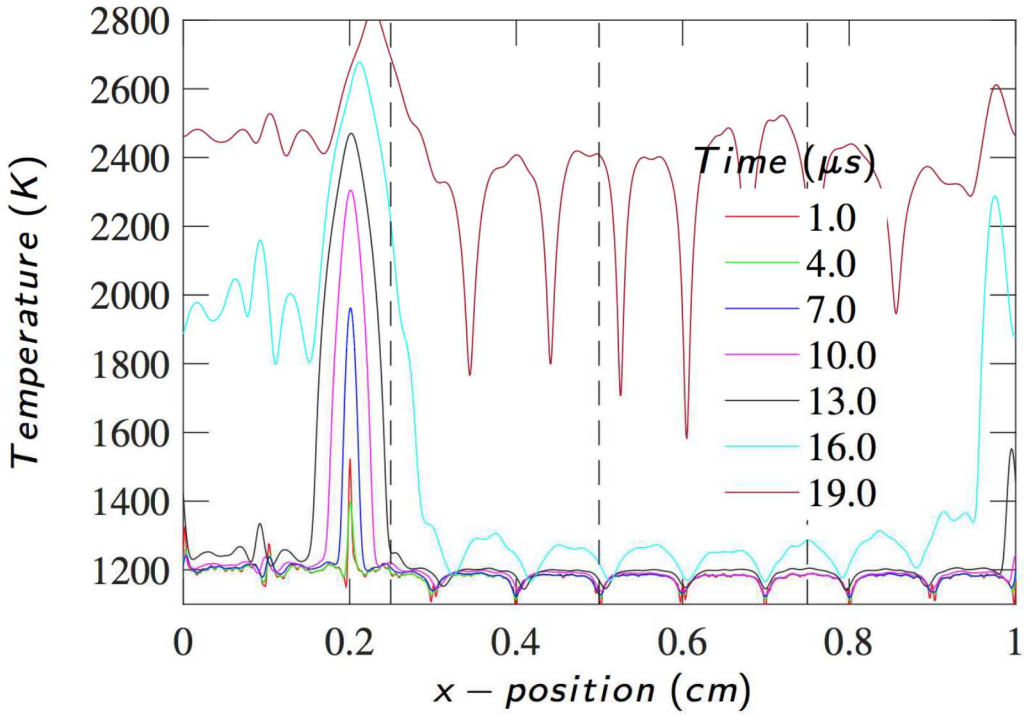

- Early ignition occurs in Region 1: spatial anomaly
- Eventually ignites in Regions 4, 2, and 3

Results

Time evolution of principal vectors in Region 1 (axes: scaled)

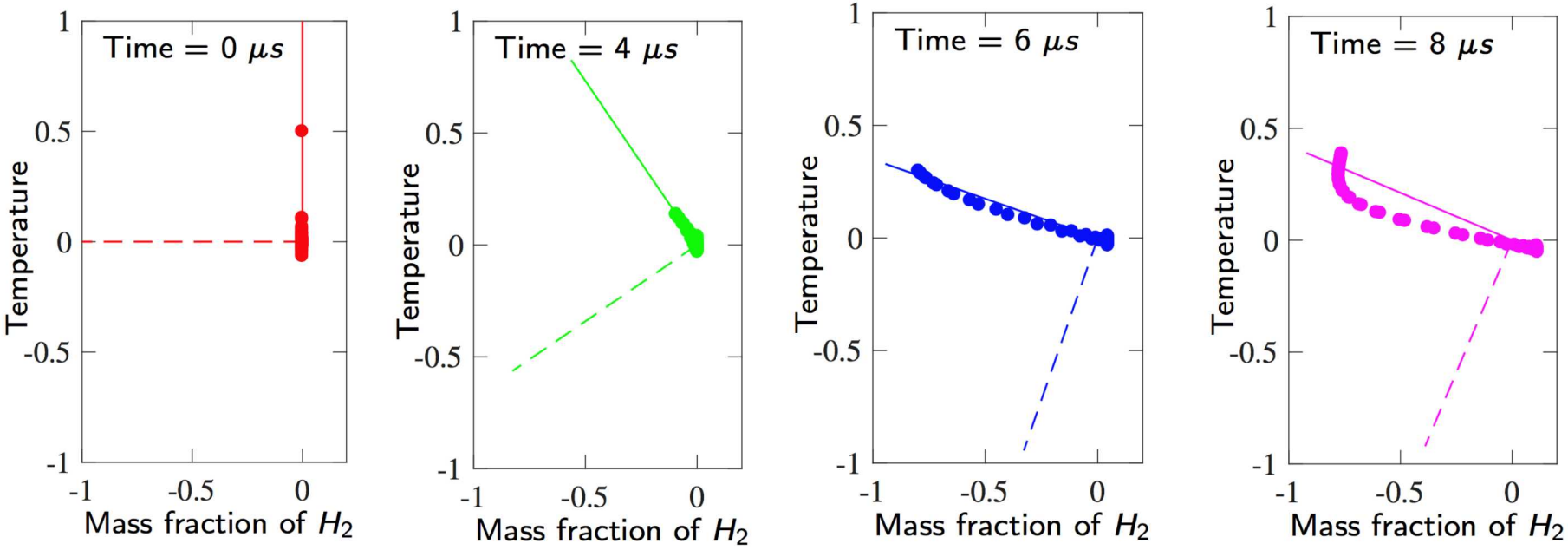

Feature moment metrics

- Number of features: N_f = 13 (12 species + temperature), index i
- Number of subdomains: N_d = 4, index j
- Number of time steps: N_t = 20, index n
- Project the principal vectors weighted by the principal values onto the features to obtain the feature moment metrics ($F_i^{j,n}$)

$$F_i^{j,n} = \frac{\sum_{k=1}^{N_f} \lambda_k \left(\hat{e}_i \cdot \hat{v}_k\right)^2}{\sum_{k=1}^{N_f} \lambda_k}$$

- $\hat{e} \cdot \hat{v}$ is effectively the i-th entry in the k-th vector $\hat{v}_k$
- Property: $\sum_{i=1}^{N_f} F_i^{j,n} = 1, \ \forall\ j, n$

Results

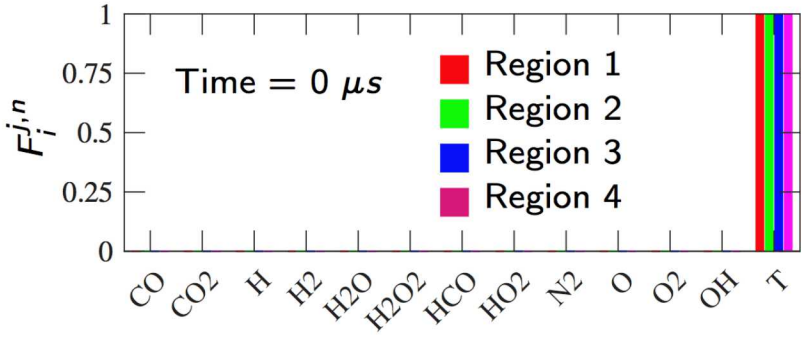

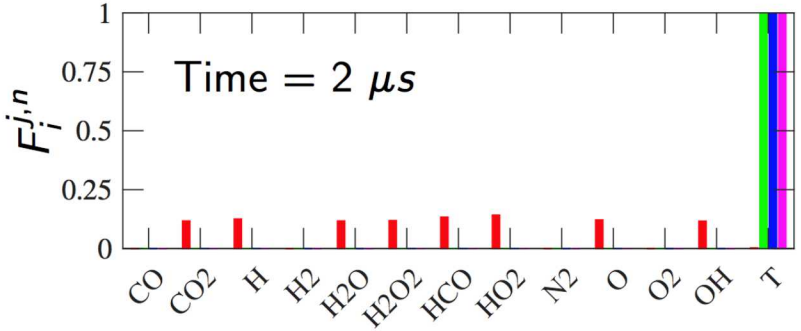

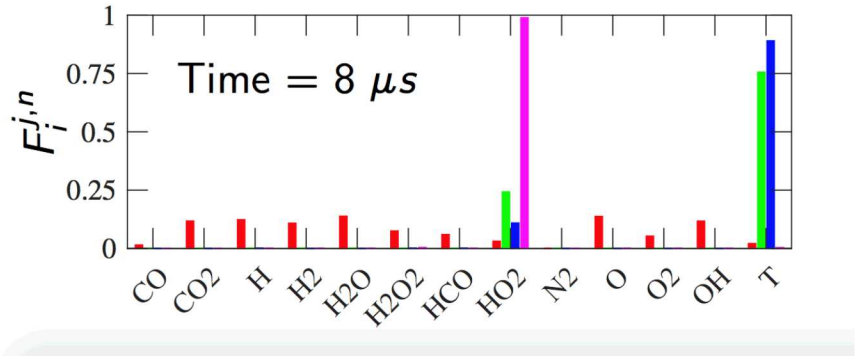

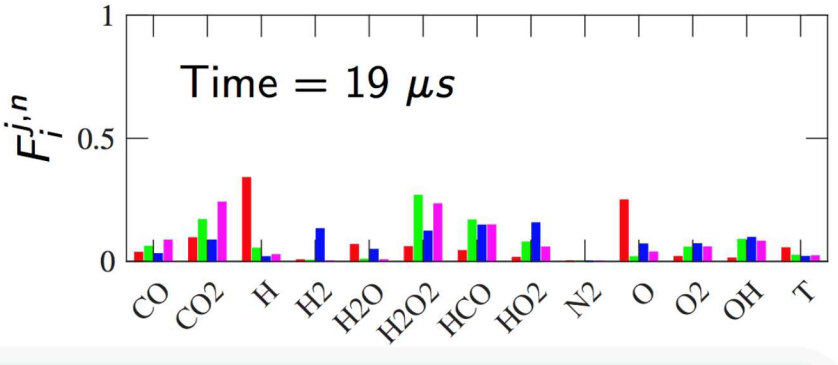

- FMMs distribute across different features when ignition (anomaly) occurs

Anomaly metrics

Identify spatial and temporal anomalies

- Statistical signature: distribution of feature moment metrics changes
- **Hellinger distance:** a symmetric measure of difference between two discrete distributions *P* and *Q*

$$D_{PQ} = \frac{1}{\sqrt{2}}\sqrt{\sum_i (\sqrt{p_i} - \sqrt{q_i})^2}$$

- **Spatial metric:** compare each FMM distribution with the average

$$M_1^n(j) = \frac{1}{\sqrt{2}}\sqrt{\sum_{i=1}^{N_f}\left(\sqrt{F_i^{j,n}} - \sqrt{\overline{F}_i^n}\right)^2}$$

- **Temporal metric:** compare FMM distribution between successive time steps

$$M_2^j(n) = \frac{1}{\sqrt{2}}\sqrt{\sum_{i=1}^{N_f}\left(\sqrt{F_i^{j,n}} - \sqrt{F_i^{j,n-1}}\right)^2}$$

Algorithm

Algorithm 1: Anomaly detection algorithm

```
   // initialization
1  N_t, N_d ← decompose data;
2  N_f ← select features;
   // time step loop
3  for n ← 1 to N_t do
       // sub-domain loop
4      for j ← 1 to N_d do
5          scale data;
6          T^{j,n} ← compute joint moment tensor;
7          matricize tensor T^{j,n} ;
8          λ_j, v_j ← perform SVD;
9          F_i^{j,n} ← compute feature importance;
10         M_1^n(j), M_2^j(n) ← compute anomaly metrics;
11     end
12     flag anomalous sub-domains;
13 end
```

Results

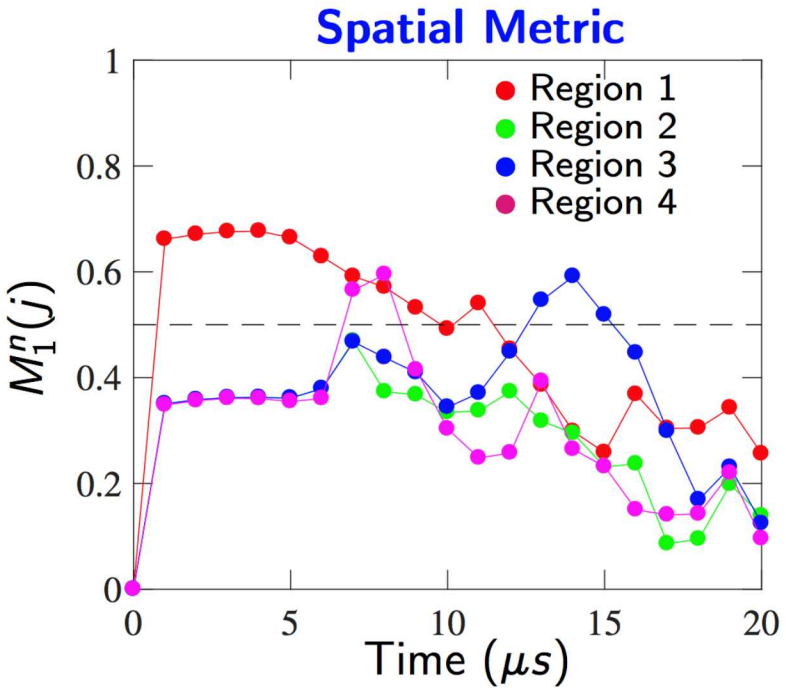

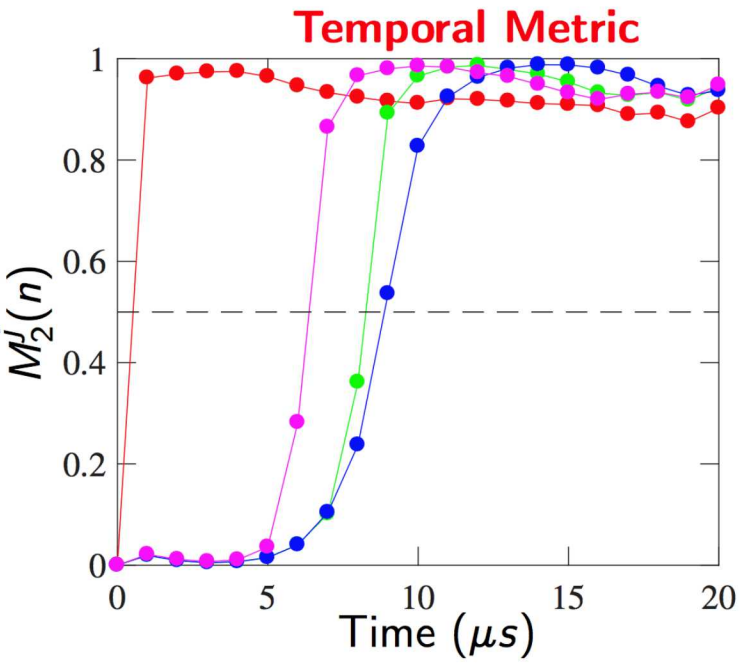

- Dash line: threshold for anomaly (=0.5)
- Anomalies detected in space and time

Forecasting

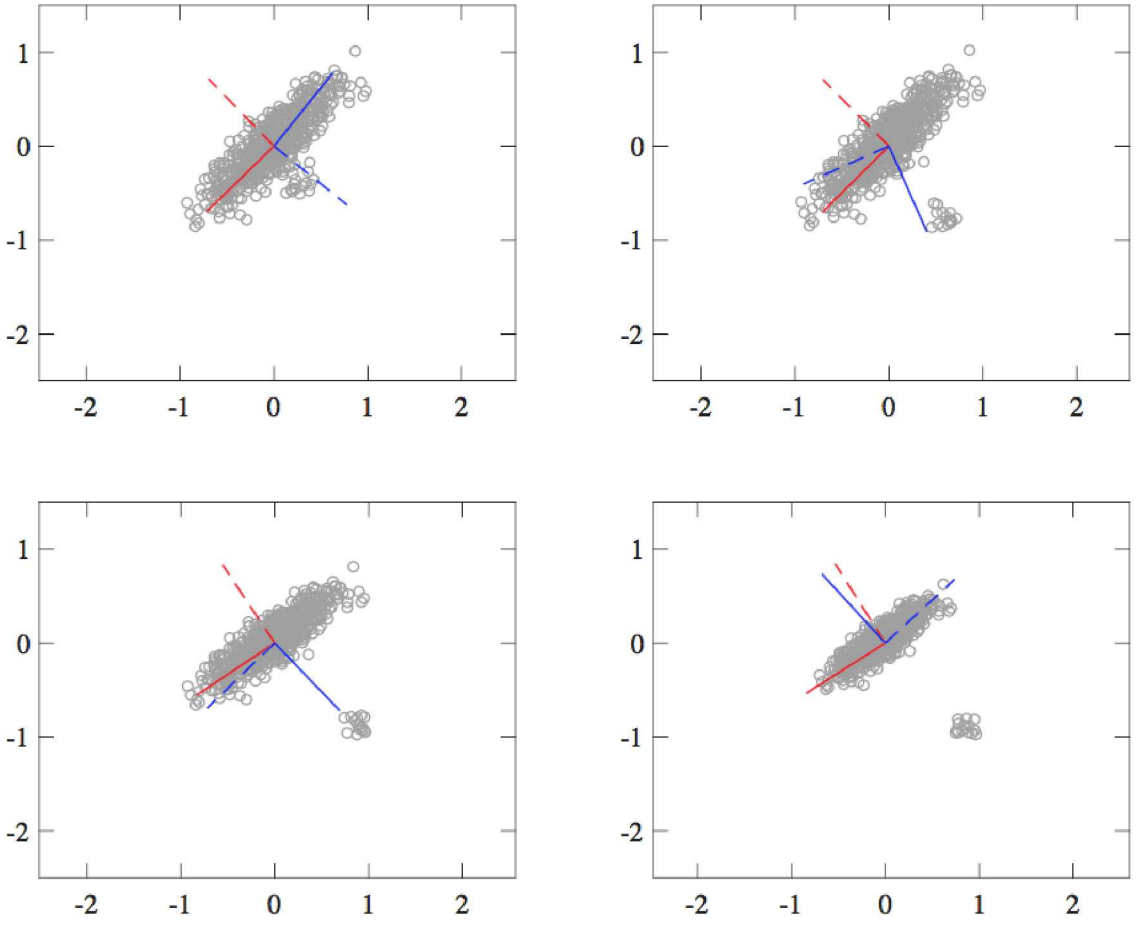

- Track the rate of change of vector orientation

Results

- Proposed an unsupervised anomaly detection algorithm
- Verified the idea using synthetic and auto-ignition data
- Future work:
  - in-situ implementation of the algorithm into the massively parallel direct numerical simulation solver (S3D)
  - evaluate scalability
  - apply the algorithm to detect anomalies in other scientific phenomena